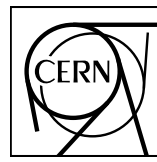


EUROPEAN ORGANIZATION FOR NUCLEAR RESEARCH



CERN-EP-2024-240
17 September 2024

Investigating charm quark energy loss in medium with the nuclear modification factor of D^0 -tagged jets

ALICE Collaboration*

Abstract

The nuclear modification factor R_{AA} of charm jets, identified by the presence of a D^0 meson among the jet constituents, has been measured for the first time in Pb–Pb collisions at a centre-of-mass energy per nucleon pair $\sqrt{s_{NN}} = 5.02$ TeV with the ALICE detector at the LHC. The D^0 mesons and their charge conjugates are reconstructed from the hadronic decay $D^0 \rightarrow K^- \pi^+$. Jets are reconstructed from D^0 -meson candidates and charged particles using the anti- k_T algorithm with jet resolution parameter $R = 0.3$, in the jet transverse momentum (p_T) range $5 < p_T^{\text{ch jet}} < 50$ GeV/ c and pseudorapidity $|\eta^{\text{ch jet}}| < 0.6$. A hint of reduced suppression in the charm-jet R_{AA} is observed in comparison to inclusive jets in central Pb–Pb collisions with a significance of about 2σ in $20 < p_T^{\text{ch jet}} < 50$ GeV/ c , suggesting the in-medium energy loss to depend on both the difference between quark and gluon coupling strength (Casimir colour-charge effect) and quark mass (dead-cone effect). The data are compared with model calculations that include mass effects in the in-medium energy loss. Among these, LIDO provides the best description of the data, highlighting the role of mass effects in interpreting the results.

© 2024 CERN for the benefit of the ALICE Collaboration.

Reproduction of this article or parts of it is allowed as specified in the CC-BY-4.0 license.

*See Appendix A for the list of collaboration members

1 Introduction

At the high energy density and temperature reached in ultrarelativistic heavy-ion collisions, the formation of a deconfined state of quarks and gluons, known as the quark–gluon plasma (QGP) [1–3], is predicted by quantum chromodynamic (QCD) calculations on the lattice [2, 4–6]. The QGP is created and studied in high-energy heavy-ion collisions at the Relativistic Heavy Ion Collider (RHIC) [7–11] and the CERN Large Hadron Collider (LHC) [3]. Heavy quarks (charm and beauty), due to their large masses, are mainly produced in hard scattering processes that occur in the early stage of the collisions, on a shorter time scale compared to the QGP formation [12, 13]. Therefore, they experience the entire evolution of the system, also considering that their thermal production and annihilation rates in the strongly interacting medium are small, even at the high temperatures and densities achieved in Pb–Pb collisions at the LHC.

Jets, i.e. collimated sprays of hadrons arising from the fragmentation of energetic partons produced in hard scattering processes, serve as effective probes for studying the microscopic interactions of partons with the QGP. Unlike single-hadron measurements, jets provide more direct information on energy and direction of the parton initiating the shower, as well as a smaller bias due to fragmentation [14]. According to QCD predictions [15–17], the parton-shower evolution of the jet in vacuum is expected to depend on the colour charge, characterised by the Casimir factor, as well as the quark mass, through the dead-cone effect, which has recently been directly measured for the first time by ALICE in pp collisions [18].

In heavy-ion collisions, high-energy partons undergo medium-induced gluon radiation and elastic scatterings [19] as a result of their interactions with the constituents of the QGP. Differences in quark mass and colour charge could be contributing factors to the difference in the energy loss between charm jets and inclusive jets, which contain a mixture of quark- and gluon-initiated jets.

Due to their large mass, heavy quarks are expected to lose less energy compared to light quarks through both collisional and radiative processes, as gluon radiation by massive quarks is suppressed (dead-cone effect) [20–22].

Such effects can be investigated, in heavy-ion collisions, with the measurement of the nuclear modification factor (R_{AA}) of jets. This factor is defined as the ratio of the p_T -differential production yield in nucleus–nucleus collisions (dN_{AA}/dp_T) and the production cross section in proton–proton collisions ($d\sigma_{pp}/dp_T$) scaled by the average nuclear overlap function, $\langle T_{AA} \rangle$

$$R_{AA} = \frac{1}{\langle T_{AA} \rangle} \frac{d^2 N_{\text{Pb-Pb}} / d\eta^{\text{ch jet}} dp_T^{\text{ch jet}}}{d^2 \sigma_{\text{pp}} / d\eta^{\text{ch jet}} dp_T^{\text{ch jet}}}, \quad (1)$$

where $\langle T_{AA} \rangle$ is estimated with Glauber model calculations [23, 24] and is related to the number of binary nucleon–nucleon collisions ($\langle N_{\text{coll}} \rangle$) and the inelastic nucleon–nucleon cross section ($\sigma_{\text{pp}}^{\text{inel}}$) according to $\langle T_{AA} \rangle = \langle N_{\text{coll}} \rangle / \sigma_{\text{pp}}^{\text{inel}}$.

Several measurements at the LHC have investigated the energy loss of charm, beauty, and light quarks and gluons via the nuclear modification of fully reconstructed D mesons, non-prompt J/ψ , and charged hadrons in Pb–Pb collisions [25–36]. The comparison with model predictions allowed for constraining the charm spatial diffusion coefficient and provided important insights into the role of radiative and collisional energy loss as well as into the hadronisation mechanism. Furthermore, the quark-mass dependence of parton energy loss was explored by comparing the R_{AA} of charm and beauty hadrons, which were either reconstructed directly or accessed through their decay products [25, 27, 35, 37, 38]. Models incorporating a quark-mass dependence of energy loss were able to describe the data. On the jet side, the measurement of radial distributions of D^0 mesons with respect to the jet axis, performed with the CMS detector [39], showed a hint of modification in Pb–Pb collisions for low- p_T D^0 mesons. This suggests charm-quark diffusion in the medium, implying a potential influence of both mass and colour charge on partonic energy loss in heavy-ion collisions. Recent measurements of the ATLAS Collaboration indicate

a lower suppression of beauty jets [40] and of photon-tagged jets (mainly produced by light quarks) [41] when compared with inclusive jets in central Pb–Pb collisions. This is evidence of a larger jet quenching in gluon jets, which are a dominant part of the inclusive jet sample at the LHC, in comparison to quark jets and it unequivocally highlights the role of the colour-charge effect.

The ALICE detector, with its excellent particle identification (PID) and tracking performance, provides the unique opportunity to tag charged-particle jets with reconstructed heavy-flavour hadrons at low p_T . Thus, it allows for the investigation of the low-jet-transverse-momentum region, where the mass effects are expected to be most pronounced.

In this paper, the yields of charm jets tagged with D^0 mesons (D^0 -tagged jets) and their nuclear modification factor in the most central (0–10%) Pb–Pb events at centre-of-mass energy $\sqrt{s_{\text{NN}}} = 5.02$ TeV are presented. This paper is organised as follows: Section 2 describes the ALICE detector and the utilised data sample; Sections 3 and 4 present details of the analysis strategy and the systematic uncertainty estimations; Section 5 reports the results compared with inclusive jet measurements and model predictions. A summary is provided in Section 6.

2 Detector and data sample

The ALICE experimental apparatus [42] consists of a central barrel (covering the pseudorapidity range $|\eta| < 0.9$) embedded in a large solenoidal magnet that provides a magnetic field of 0.5 T, parallel to the beams axis. It also includes a forward muon spectrometer ($-4 < \eta < -2.5$) and a set of detectors at forward and backward rapidity used for triggering, background rejection, and event characterisation.

The central-barrel detectors employed in this paper for charged-particle reconstruction and identification at midrapidity are the Inner Tracking System (ITS) [43], the Time Projection Chamber (TPC) [44], and the Time-Of-Flight detector (TOF) [45]. The ITS consists of six layers of silicon detectors used for tracking charged particles and reconstructing primary and secondary vertices. The TPC serves as the main tracking detector and provides particle identification through the measurement of the particle specific energy loss (dE/dx) in the detector gas. Complementary particle identification information is obtained from the TOF, which measures the flight time of charged particles from the interaction point to the detector.

The results reported in this paper were obtained using the data sample collected during the 2018 LHC Pb–Pb run at centre-of-mass energy $\sqrt{s_{\text{NN}}} = 5.02$ TeV. Events were selected using a minimum bias (MB) trigger provided by the V0 detectors [46], which consist of two arrays of 32 scintillators each, covering the full azimuthal angle in the pseudorapidity ranges of $-3.7 < \eta < -1.7$ (V0C) and $2.8 < \eta < 5.1$ (V0A). An additional trigger class, based on the online event selection provided by the V0 signal amplitude, was used during the data taking to enrich the sample of central collisions considered in this analysis. Events arising from the interactions of the beams with residual gas in the vacuum pipe were rejected offline using the timing information from the V0 detector and the Zero Degree Calorimeter (ZDC) [47]. Only the events with a primary vertex reconstructed within ± 10 cm from the nominal centre of the detector along the beam axis were considered in the analysis. The centrality estimator is defined in terms of percentiles of the hadronic Pb–Pb cross section, using the sum of the V0 signal amplitudes, as described in detail in Ref. [43]. In the present analysis, only the 10% most central collisions are used (0–10% centrality class). The corresponding average nuclear overlap function is $\langle T_{\text{AA}} \rangle = 23.26 \pm 0.17 \text{ mb}^{-1}$ [48, 49] and the total number of analysed events is about $N_{\text{events}} = 100 \times 10^6$, corresponding to an integrated luminosity of $L_{\text{int}} = 130.5 \pm 0.5 \mu\text{b}^{-1}$. The data used for the measurement of the pp reference in the calculation of the R_{AA} is the same as used in Ref. [50].

The Monte Carlo samples used for the corrections in this analysis were generated by simulating pp collisions containing a $c\bar{c}$ or a $b\bar{b}$ pair with PYTHIA 8 [51] (Monash 2013 tune [52]). The charged-

particle multiplicity and detector occupancy observed in data [53] were simulated superimposing an underlying event generated with HIJING 1.36 [54]. The generated-level particles from these simulations were passed through a particle transport and detector-response simulation of the entire ALICE apparatus based on GEANT3 [55].

3 Analysis Strategy

The analysis closely follows the procedure described in detail in the ALICE studies of charm jets tagged with D^0 mesons [50]. It consists of three main parts: (i) reconstruction of jets tagged by the presence of a D^0 meson; (ii) extraction of the raw yields of D^0 -tagged jets; (iii) correction for the reconstruction efficiency of the D^0 jets, subtraction of the feed-down contribution from D^0 mesons coming from beauty decays, and correction for the detector-related effects and underlying-event fluctuations.

A major challenge in jet reconstruction in central heavy-ion collisions compared to pp collisions is the fluctuation of the underlying event, which is a background to the reconstructed jet. These fluctuations significantly affect the jet transverse momentum. To account for these background fluctuations and detector effects, the data was corrected using a deconvolution procedure (unfolding). This correction involved constructing a response matrix that maps the D^0 -jet p_T at the generated level, simulated using PYTHIA 8 for pp collisions, to the detector-level spectrum. The matching between generated and detector-level D^0 jets was achieved by requiring the identification of the same D^0 meson among their constituents. To ensure a realistic representation of the heavy-ion environment, detector-level particles were embedded into real Pb–Pb data to simulate the background accurately.

3.1 D^0 -meson selection and jet reconstruction

The D^0 and \overline{D}^0 mesons were reconstructed via the hadronic decay channel $D^0 \rightarrow K^- \pi^+$ (and its charge conjugate) with branching ratio $BR = 3.950 \pm 0.031\%$ [15]. D^0 mesons produced either directly from charm-quark fragmentation or from decays of directly-produced excited charm hadron states are referred to as prompt D^0 mesons, while those originating from decays of beauty hadrons are termed non-prompt D^0 mesons. The selection strategy, described in detail in Refs. [56] and [25], exploited the displaced topology of the decay and made use of the particle identification capabilities of the TPC and TOF to identify the decay particles of the D^0 mesons in the pseudorapidity interval $|\eta_D| < 0.9$.

Charm-jet reconstruction was performed using a track-based procedure with the FastJet [57] anti- k_T clustering algorithm [58] with resolution parameter $R = 0.3$. This parameter was chosen in order to keep under control the jet background fluctuations, which increase for large R , while the jet's characteristics are not completely dominated by the jet core, which happens for small R . The jet reconstruction was carried out using the p_T -recombination scheme [59], in the kinematic range $5 < p_T^{\text{ch jet}} < 50 \text{ GeV}/c$. Charged particles were required to have $p_T > 150 \text{ MeV}/c$ and $|\eta| < 0.9$. To ensure that the entire jet was contained within the detector acceptance, jets were required to have their axes within the pseudorapidity range of $|\eta| < 0.9 - R$.

At low momenta, the D^0 decay products may be emitted at angles larger than the defined jet cone size. To address this issue and ensure that the pion and kaon from the D^0 decay were assigned to the same jet, they were removed from the set of charged-particle tracks before the jet reconstruction and their four-momenta were replaced by that of the D^0 candidate. A charm jet was identified when a D^0 -meson candidate in the transverse momentum range $3 < p_{T,D} < 36 \text{ GeV}/c$ was found among its constituents. This procedure was repeated for each D^0 -meson candidate in the event, where the decay products of only one candidate were replaced at a time.

Measuring jets in heavy-ion collisions down to low transverse momentum, such as $5 \text{ GeV}/c$, is particularly challenging due to the large background from the underlying event and its fluctuations [60]. At low p_T , a large fraction of the reconstructed jets is not related to a hard scattering process. This background

source dominates the low jet- p_T region (below 20 GeV/c). Moreover, independently of the p_T interval, all reconstructed jets can include tracks from the underlying event, i.e. particles not originating from the fragmentation of the hard-scattered parton that initiated the jet. To account for the background coming from the underlying event, the area-based method was employed, following the approach described in Refs. [61, 62]. This method estimates the average additive contribution to the jet momentum on a jet-by-jet basis. The underlying background momentum density, ρ^{ch} , was estimated event-by-event using the median of $p_{T,\text{raw}}^{\text{ch jet}}/A_{\text{raw}}^{\text{ch jet}}$, where $p_{T,\text{raw}}^{\text{ch jet}}$ is the uncorrected jet transverse momentum and $A_{\text{raw}}^{\text{ch jet}}$ is the area of jets reconstructed with the k_T algorithm [63]. The two leading jets were removed from the calculation of ρ^{ch} . The signal anti- k_T jets were then corrected by subtracting the median of the jet transverse momentum density multiplied by the jet area: $p_{T,\text{corr}}^{\text{ch jet}} = p_{T,\text{raw}}^{\text{ch jet}} - \rho^{\text{ch}} A_{\text{raw}}^{\text{ch jet}}$.

3.2 Extraction of D⁰-tagged jet raw yields

The raw yield of D⁰ jets was determined through an invariant-mass analysis of the D⁰-meson candidates used for tagging the charm-jet candidates. The analysis was performed in different intervals of D⁰-meson transverse momentum ranging from 3 to 36 GeV/c. For each $p_{T,D}$ interval, the invariant-mass distribution of the D⁰-meson candidates was fitted with a function consisting of a Gaussian function to represent the signal and an exponential function to account for the combinatorial background [56].

When the two tracks forming a D⁰ candidate are compatible with both the kaon and pion hypothesis, the candidate can be identified both as a D⁰ and as a \bar{D}^0 , leading to an irreducible correlated background, which is referred to as reflections [56, 64]. The contribution of residual D⁰-meson reflections, which were not rejected by particle identification, were considered in the fit by including a template composed of the sum of two Gaussian functions. The centroids and widths of these Gaussian functions were fixed to the values based on a fit to the invariant mass distributions of reflections derived from the simulation. The ratio between the reflected signal and the D⁰-meson yield was also fixed to the value obtained from the simulations.

The yield of D⁰-meson-tagged jet candidates was determined by dividing the corresponding D⁰ invariant-mass range in two sub-samples within each $p_{T,D}$ interval: a *peak region* corresponding to candidates with $|m_{\text{inv}} - m_{\text{fit}}| < 2\sigma_{\text{fit}}$ (where m_{fit} and σ_{fit} are the mean and width of the Gaussian component of the fit, respectively) and a *sideband region* consisting of candidates with $4\sigma_{\text{fit}} < |m_{\text{inv}} - m_{\text{fit}}| < 8\sigma_{\text{fit}}$. The jet p_T distribution associated with the D-meson candidates in the sideband region was normalised to the integral of the background in the peak region and then subtracted from the jet p_T distribution in the peak region to obtain the raw yield of D⁰ jets.

3.3 Corrections of D⁰-tagged-jet raw yields

The raw yields of D⁰-tagged jets extracted using the invariant mass method required corrections to account for the limited detector acceptance and the reconstruction efficiency of D⁰ mesons. These corrections are described in detail in Refs. [50, 65]. After the removal of non-prompt D⁰ meson contributions, the raw yield is unfolded to correct for the detector finite resolution and jet background fluctuations.

First, the raw yields obtained in different intervals of $p_{T,D}$ were corrected for the product of the acceptance and the reconstruction efficiency of prompt D⁰ mesons associated to jets that pass the acceptance and $p_T^{\text{ch jet}}$ selection, $\epsilon^{\text{c} \rightarrow \text{D}^0}(p_{T,D})$. This correction factor took into account the probability of detecting and reconstructing jets containing prompt D⁰ mesons within the specified $p_{T,D}$ intervals and the jet cone radius.

A fraction of the reconstructed D⁰-meson-tagged jets originates from the fragmentation of beauty quarks, where a beauty hadron decays into a D⁰ meson. The contribution from beauty jets was estimated using generated templates of non-prompt D⁰-jet p_T distributions obtained with NLO pQCD calculations of POWHEG [66–69] coupled to the PYTHIA 6 [70] parton shower. The templates were generated with

specific configurations in POWHEG, such as a b-quark mass $m_b = 4.75 \text{ GeV}/c^2$, the renormalisation (μ_R) and factorisation (μ_F) scales set to the quark transverse mass $\mu_R = \mu_F = \sqrt{m_b^2 + p_T^2}$, and the use of parton distribution functions (PDF) from the CT10NLO [71] set using the LHAPDF6 [72] interpolator.

The non-prompt-D⁰-jet yield estimated by the simulation ($N_{\text{POWHEG}}^{b \rightarrow D^0}$) was weighted by the ratio of the efficiencies of non-prompt and prompt D⁰-jets ($\epsilon^{b \rightarrow D^0}(p_{T,D})/\epsilon^{c \rightarrow D^0}(p_{T,D})$) in order to be comparable with $\epsilon^{c \rightarrow D^0}$ -scaled inclusive D⁰-jet distributions from data. As a next step, the simulated non-prompt D⁰-jet distribution was smeared with the non-prompt response matrix ($\text{RM}_{b \rightarrow D^0}$) in order to take into account the effect of the detector on the jet momentum resolution. The spectrum was also corrected for the kinematic efficiency, which accounts for the limited transverse momentum ranges of the response matrix in the generated ($\epsilon_{\text{kine}}^{\text{gen}}$) and reconstructed ($\epsilon_{\text{kine}}^{\text{rec}}$) axes. Additionally, the measured nuclear modification factor of non-prompt-D⁰ mesons ($R_{AA}^{b \rightarrow D^0}$) [27] was used to weight the non-prompt D⁰-jet p_T spectrum. This assumes that the non-prompt D⁰-jet R_{AA} is dominated by the non-prompt D⁰. This assumption is supported by the expected hard fragmentation of the bottom quark. As a result, the yield of prompt-D⁰ jets, N^c , was determined as follows

$$N^c(p_T^{\text{ch jet}}) = N^{c+b}(p_T^{\text{ch jet}}) - N^b(p_T^{\text{ch jet}}), \quad (2)$$

where the contribution of non-prompt D⁰-jet, N^b , was estimated using the following formula

$$N^b(p_T^{\text{ch jet}}) = \frac{1}{\epsilon_{\text{kine}}^{\text{rec}}} \left[\sum_{p_{T,D}} \text{RM}_{b \rightarrow D^0}(p_T^{\text{ch jet}}, p_{T,D}) \otimes \sum_{p_{T,D}} \frac{\epsilon^{b \rightarrow D^0}(p_{T,D})}{\epsilon^{c \rightarrow D^0}(p_{T,D})} R_{AA}^{b \rightarrow D^0}(p_{T,D}) \epsilon_{\text{kine}}^{\text{gen}} N_{\text{POWHEG}}^{b \rightarrow D^0}(p_T^{\text{ch jet}}, p_{T,D}) \right]. \quad (3)$$

The contribution of non-prompt D⁰ jets varies between 20% and 24% of the inclusive yields depending on the jet p_T .

Finally, the measured D⁰-jet yield was unfolded with an iterative method based on Bayes' theorem [73] as implemented in the RooUnfold package [74]. The chosen number of iterations was eight, based on optimal convergence. Both the prompt and non-prompt-D⁰-jet response matrices were corrected for the kinematic efficiency.

To verify the stability of the unfolding and the choice of the number of iterations, the unfolded spectra were folded back and compared to the original data, showing good agreement in all the cases.

4 Systematic uncertainties

The systematic uncertainty associated to the measurement has several independent sources. These sources were identified as coming from: (i) yield extraction, (ii) D⁰-jet reconstruction efficiency, (iii) feed-down subtraction, (iv) tracking efficiency, (v) unfolding, and (vi) branching ratio.

The uncertainty on the yield extraction procedure, described in Section 3.2, was evaluated by varying the fit approach. In particular, the fit was repeated using different functions to describe the background, varying the fit range, fixing the mean of the Gaussian term describing the signal peak to the nominal value of the D⁰-meson mass or fixing the Gaussian width to the value obtained from Monte Carlo studies. The standard deviation calculated from all variations with respect to the default set of parameters was used as systematic uncertainty. The uncertainties obtained with this procedure increase from 5% at low jet transverse momentum to 6% at higher jet p_T .

The possible differences in the topological variable distributions between Monte Carlo and data can

affect the D^0 -jet reconstruction efficiency. The related systematic uncertainty was evaluated by extracting the raw-jet p_T spectrum with tighter and looser topological selections of the D^0 -jet candidates. The corresponding systematic uncertainty varies from 5% at the low jet transverse momentum up to 14% in the highest p_T interval (30–50 GeV/ c).

The uncertainty on the subtraction of the beauty feed-down contribution was quantified by varying the factorisation and renormalisation scales, the beauty-quark mass, and the PDF in the generated POWHEG + PYTHIA 6 templates of non-prompt- D^0 jets [75]. The largest deviations among all variations were used as systematic uncertainties, resulting in a value of 7–8% depending on the jet p_T . An additional contribution to this uncertainty comes from the systematic uncertainty related to the assumption on the nuclear modification factor $R_{AA}^{b \rightarrow D^0}$. It was estimated by assuming different values of the non-prompt- D^0 nuclear modification factor and recalculating the non-prompt D^0 -jet yield N^b . The difference between the variations and the default spectrum was used as systematic uncertainty. The uncertainty ranges from 6% to 8% in jet p_T kinematic interval.

The uncertainties on the track reconstruction efficiency can impact the jet momentum resolution and D^0 -jet reconstruction efficiency. The systematic uncertainty on the reconstruction efficiency of a single track was estimated to be 4% [76]. To evaluate its impact, a response matrix was built by randomly rejecting 4% of the reconstructed tracks (artificially decreasing the tracking efficiency). This response matrix was used to unfold the measurement and the difference with respect to the results obtained with the default response matrix was considered as systematic uncertainty. This uncertainty varies from 0.5% in the 5–6 GeV/ c jet p_T range up to 10% in the 30–50 GeV/ c jet- p_T interval.

The systematic uncertainties due to the unfolding procedure were evaluated by studying three independent aspects of the Bayesian unfolding method. First, the regularisation parameter was varied by ± 1 iteration. These two variations were compared to the unfolded distribution obtained using the default parameter and the largest deviations were used as systematic uncertainty. Second, the shape of the prior spectrum of the D^0 -jet transverse-momentum distribution in the response matrix was also varied. The default shape was taken from POWHEG+PYTHIA 6 simulations and the variation used was from PYTHIA 8. The observed difference was adopted as systematic uncertainty. Third, the lower limit of the kinematic range of the measurement was also varied and, after unfolding, the spectrum was compared to the default range and the relative deviation was used as systematic uncertainty. The combined systematic uncertainties from unfolding range from 8% at low jet p_T to 16% in the 30–50 GeV/ c interval.

The systematic uncertainties arising from the sources that affect the raw jet- p_T spectrum (such as yield extraction, kinematic and topological selections, and feed-down subtraction) were propagated to the final D^0 -jet yield by unfolding the upper and lower bands of the combined systematic uncertainty. These were then combined in quadrature with the systematic uncertainties affecting the correction of the reconstructed jet momentum (including single-particle tracking efficiency and unfolding). This resulted in a combined systematic uncertainties for D^0 jets that varies from 15% in the 5–6 GeV/ c jet p_T range up to 52% in the 30–50 GeV/ c interval.

In the evaluation of the nuclear modification factor, the systematic uncertainties associated with the D^0 -jet yield in Pb–Pb collisions and the reference cross section in pp collisions were treated as uncorrelated, with the exception of the uncertainty related to the branching ratio (BR), which cancels out in the ratio, and the feed-down that was considered as partially correlated between pp and Pb–Pb collisions. The contributions of the uncertainties on the luminosity determination in pp collisions, and the $\langle T_{AA} \rangle$ estimated with the Glauber model are common across all the transverse-momentum intervals and therefore contribute to a normalisation uncertainty on the R_{AA} , which is shown separately from the other sources when displaying the results.

5 Results and discussion

The transverse-momentum differential yields of charm jets tagged with prompt D^0 mesons in central Pb–Pb collisions at $\sqrt{s_{\text{NN}}} = 5.02$ TeV were calculated using the following equation (4), with the measured yields corrected according to the procedure described in Section 3:

$$\frac{d^2N}{d\eta^{\text{ch jet}} dp_T^{\text{ch jet}}} = \frac{1}{N_{\text{events}}} \frac{1}{\text{BR}} \frac{N(p_T^{\text{ch jet}})}{\Delta\eta^{\text{ch jet}} \Delta p_T^{\text{ch jet}}}, \quad (4)$$

where N_{events} is the number of events, BR is the branching ratio of the considered D^0 decay channel, $N(p_T^{\text{ch jet}})$ is the measured yield in each interval of transverse momentum, $\Delta\eta^{\text{ch jet}}$ is the pseudorapidity interval of D^0 jets and $\Delta p_T^{\text{ch jet}}$ is the width of the p_T interval.

Figure 1 displays the measured yields of charm jets tagged with a prompt D^0 meson in the transverse momentum interval $5 < p_T^{\text{ch jet}} < 50$ GeV/ c for central (0–10%) Pb–Pb collisions at a centre-of-mass energy of $\sqrt{s_{\text{NN}}} = 5.02$ TeV, along with the reference yields from pp collisions [50]. The reference yields in pp collisions were computed as the product of the average nuclear overlap function $\langle T_{\text{AA}} \rangle$ and the D^0 -jet p_T -differential cross section $d\sigma_{\text{pp}}/dp_T$. In both collision systems, the charm jets were required to contain a prompt D^0 as one of their constituents, reconstructed in the kinematic interval $3 < p_{T,D} < 36$ GeV/ c . This requirement allowed for the reconstruction of D^0 -tagged jets with low transverse momentum. The measured yields in Pb–Pb collisions exhibit a clear suppression of the D^0 -jet production yield compared to the reference yields in pp collisions. The nuclear modification factor (R_{AA}) of prompt-

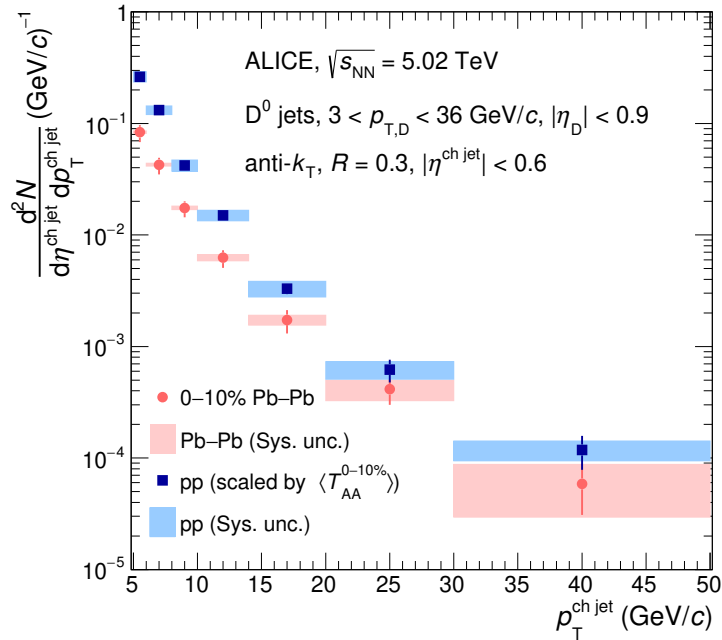


Figure 1: Transverse-momentum differential yields of charm jets tagged with prompt D^0 mesons in central (0–10%) Pb–Pb collisions at $\sqrt{s_{\text{NN}}} = 5.02$ TeV (red markers) and cross section in pp collisions at $\sqrt{s} = 5.02$ TeV (blue markers) scaled by the nuclear overlap function $\langle T_{\text{AA}} \rangle$ for the considered centrality interval. The vertical lines are the statistical uncertainties and the filled squares are the systematic uncertainties.

D^0 jets was computed, based on Eq. (1), using the transverse momentum differential yield measured in Pb–Pb collisions and the pp reference at the same centre-of-mass energy [50].

The resulting R_{AA} of charm jets tagged with prompt D^0 mesons is shown in Fig. 2. The value of R_{AA}

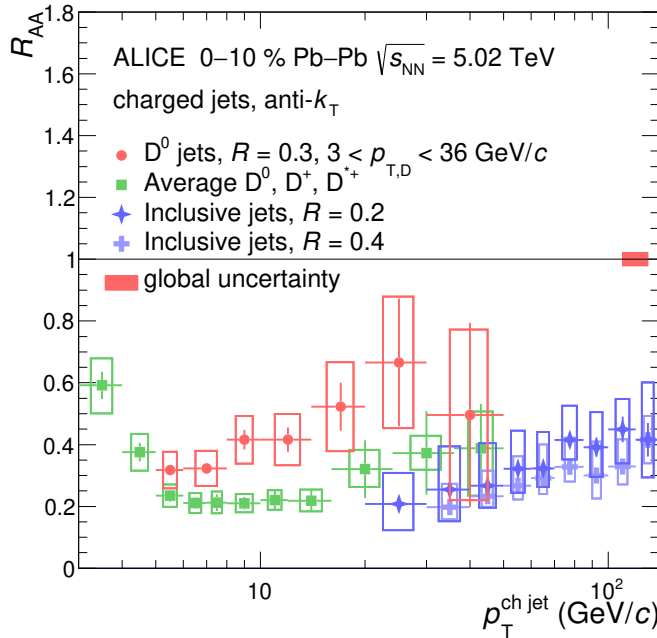


Figure 2: Nuclear modification factor of D^0 jets (red markers), inclusive jets with resolution parameter $R = 0.2$ (light blue) and $R = 0.4$ (blue markers) [77], and averaged D^0 , D^+ , D^{*+} mesons [56] (green markers). Statistical and systematic uncertainties are shown as vertical error bars and boxes, respectively. The global uncertainty originated from the $\langle T_{AA} \rangle$ normalisation and the luminosity is displayed as a box around unity.

increases as a function of jet p_T . It varies from about 0.32 in the lowest jet- p_T interval to 0.5 in the highest jet- p_T interval. This indicates a strong suppression of D^0 -jet production in central (0–10%) Pb–Pb collisions at $\sqrt{s_{NN}} = 5.02$ TeV.

Figure 2 shows the comparison of D^0 -jet R_{AA} to the R_{AA} of inclusive charged-particle jets with $R = 0.2$ and with $R = 0.4$ [77]. The two inclusive-jet R_{AA} measurements are compatible between each other within systematic uncertainties, with the R_{AA} for $R = 0.4$ being systematically lower. The R_{AA} measurement for $R = 0.3$ is not available, but it is reasonable to expect that it should lie between the two measurements. Due to its broader kinematic range, only the measurement with $R = 0.2$ will be considered from this point onward. In the overlapping jet transverse momentum region ($20 < p_T^{\text{ch jet}} < 50$ GeV/ c), the inclusive jet R_{AA} is lower than the D^0 -jet R_{AA} , suggesting a reduced suppression of charm jets tagged with D^0 mesons as compared to inclusive jet. The statistical significance of the difference is about 2.1σ in the transverse momentum range $20 < p_T^{\text{ch jet}} < 30$ GeV/ c and 1.8σ in the entire transverse momentum region of the overlap between the two measurements. The figure shows also the comparison with the nuclear modification factor (average of D^0 , D^+ , and D^{*+}) taken from Ref. [56]. Despite the difficulty in assessing a momentum scale to properly compare the jet and the single hadron measurements, it is remarkable to observe that D^0 jets and D mesons show similar magnitudes of suppression at similar p_T . The minimum $p_{T,D}$ is 3 GeV/ c , which is a lower limit for all D^0 jets in this measurement. The upper limit of the first D^0 -jet $p_T^{\text{ch jet}}$ interval (5–6 GeV/ c) also limits its highest $p_{T,D}$. The R_{AA} in this D^0 -jet interval is consistent with the D^0 R_{AA} in the range $4 < p_{T,D} < 6$ GeV/ c .

In evaluating the comparison between inclusive jets and D^0 jets, the steepness of the transverse-momentum differential yields in pp collisions, which were used as the reference for computing the R_{AA} , should be taken into account. The momentum shift of inclusive and D^0 jets due to the energy loss could differ due to the different steepness of their transverse-momentum spectrum and introduce a bias in the comparison of the two R_{AA} measurements.

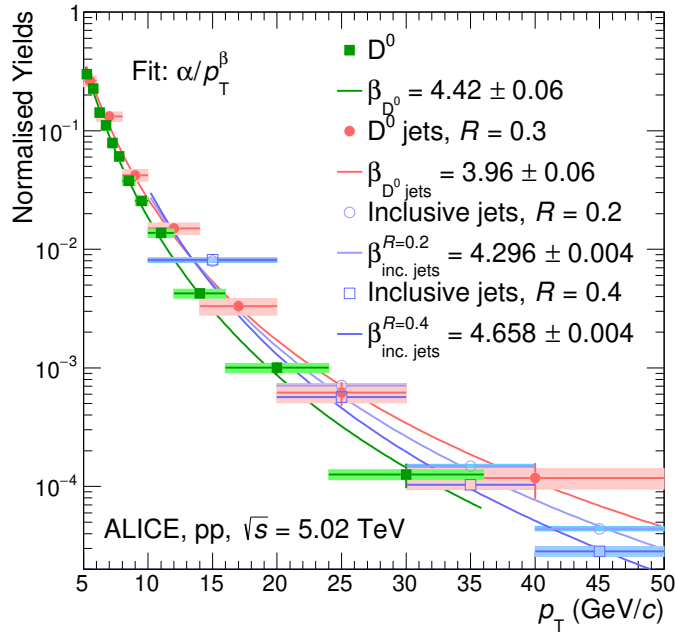


Figure 3: Transverse momentum distributions of D⁰ mesons (green markers) [64], inclusive jets with jet resolution parameter 0.2 (light blue) and 0.4 (blue markers) [78], and D⁰ jets (red markers) in pp collisions at $\sqrt{s} = 5.02$ TeV (see text for details about the normalisation). Statistical and systematic uncertainties are shown as vertical error bars and boxes, respectively. The function α/p_T^β was fitted to each of the distributions (solid lines) to compare their steepness.

Figure 3 presents the p_T -differential yields of D⁰ mesons [64], D⁰-tagged jets [50], and inclusive jets with $R = 0.2$ and $R = 0.4$ [78] measured in pp collisions at $\sqrt{s} = 5.02$ TeV and normalised to their integral in given p_T intervals. The D⁰ distribution was normalised in such a way that it has the same integral in the interval 5 to 6 GeV/c as the D⁰-tagged jet distribution. The same was done for the inclusive-jet distributions in the interval 10 to 50 GeV/c. Each transverse momentum distribution was fitted using a function α/p_T^β , where α is a parameter that accounts for the normalisation of the distributions, and β quantifies the steepness of the function. Both statistical and systematic uncertainties were considered for the fit. For the D⁰-meson and inclusive-jet transverse momentum spectra in pp collisions, it was found that $\beta_{D^0} = 4.42 \pm 0.06$, $\beta_{inc. jets}^{R=0.2} = 4.296 \pm 0.004$, and $\beta_{inc. jets}^{R=0.4} = 4.658 \pm 0.004$, which show that these are steeper transverse momentum distributions in comparison to D⁰ jets with $\beta_{D^0 jets} = 3.96 \pm 0.06$. However, even assuming an hypothetical scenario where 80% of the jets have a 10 GeV/c shift to lower p_T , the difference in the steepness between inclusive jets and jets tagged with a D⁰ could account for up to a 9% difference between their nuclear modification factors, thus is not sufficiently large to explain the observed differences in their respective R_{AA} .

In Fig. 4, the nuclear modification factors of both D⁰-tagged jets and inclusive jets are compared to calculations from different theory models, namely Dai et al. [80], JETSCAPE [79] (left panel) and to LIDO [81, 82] model (right panel).

The calculation by Dai et al. [80] is based on a Langevin transport model, which describes the evolution of heavy quarks and their collisional energy loss, as well as a higher-twist description of radiative energy loss for both heavy and light partons. This model also includes the dead-cone effect for heavy quarks and utilises a (2+1)-dimensional viscous hydrodynamic medium with averaged initial conditions. The model uses a fixed jet transport parameter (proportional to the local parton density in the medium) $\hat{q}_0 = 1.2$ GeV²/fm and varies its value ($1 < \hat{q}_0 < 1.5$ GeV²/fm) to estimate the uncertainties of the model

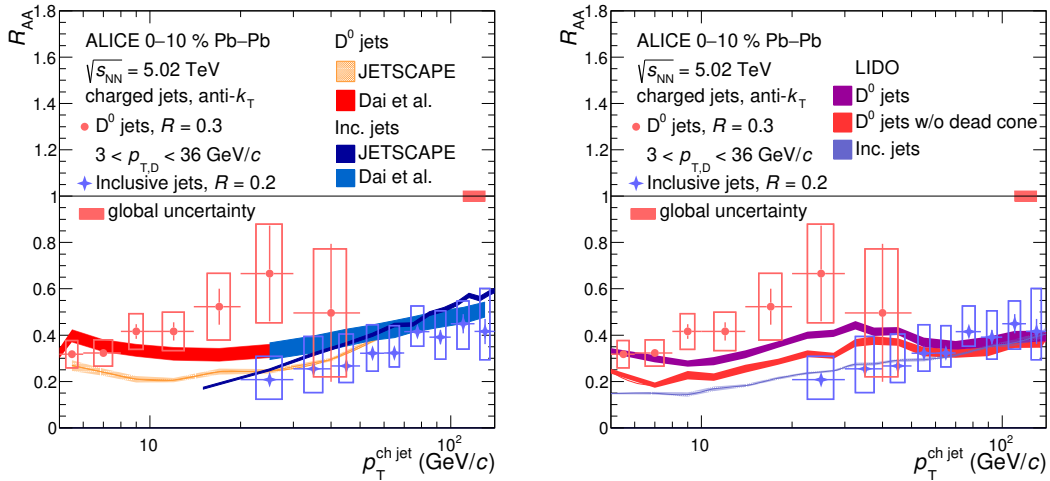


Figure 4: Left: comparison of the nuclear modification factor of D^0 jets (and inclusive jets) with predictions from JETSCAPE [79] and Dai et al. [80]. The bands of the theory curves represent the systematic uncertainties on the model predictions. Right: comparison to the LIDO [81, 82] predictions for D^0 jets with and without dead-cone effect and predictions for inclusive jets.

predictions. It reproduces the measured inclusive jet R_{AA} , consistently lying on the upper edge of the systematic uncertainties of the data points. However, it tends to underestimate the nuclear modification factor of D^0 -tagged jets for $p_T^{ch\ jet} > 12$ GeV/ c .

The JETSCAPE model [79] includes a modification of the parton shower due to the interaction with the medium using MATTER [83] at high parton virtuality, and LBT [84] at low parton virtuality. JETSCAPE severely underestimates the R_{AA} of D^0 jets, while showing good agreement with the inclusive jet R_{AA} measurement.

LIDO is a partonic transport model that incorporates heavy-quark scatterings with medium partons using matrix elements calculated in perturbative QCD. It describes the transport of heavy quarks between scatterings through a Boltzmann type equation, including both elastic collisions and medium-induced parton radiation. The transport coefficients in LIDO are calibrated using a Bayesian analysis to match the measured single-inclusive nuclear modification factors of light-flavour hadrons and D mesons at the LHC and RHIC [85]. The model introduces the parameter μ_{min} to control the coupling between the jet and the medium, based on measurements of the R_{AA} of B and D mesons. The value of this parameter is proportional to the temperature of the QGP, T . LIDO predictions, shown in the right panel of Fig. 4, were obtained with $\mu_{min} = 1.8\pi T$ and demonstrate the best agreement with the data in terms of the shape and trend for both inclusive jets and D^0 jets.

Predictions for inclusive jets down to $p_T = 5$ GeV/ c (compatible with the minimum p_T of the D^0 -tagged jet measurement) confirm the larger suppression of inclusive jets also at low p_T . Moreover, the result obtained without including the dead-cone effect in the calculations are also shown to single out the quark-mass effect in this model.

The absence of dead-cone effect for the charm jets results in a larger suppression of the nuclear modification factor for $p_T^{ch\ jet} < 50$ GeV/ c , pointing towards a significant role of the mass effect in this kinematic region. The dead-cone effect becomes less relevant for $p_T^{ch\ jet} > 50$ GeV/ c , where the model predictions for charm jets and inclusive jets are extended up to $p_T = 200$ GeV/ c and result to be compatible. This observation corroborates the mass-hierarchy in energy loss, as evidenced also by the comparison of the nuclear modification factors of beauty-originated hadrons and charm-originated hadrons [27, 37]. The residual difference between the model curves of D^0 -tagged jets without dead-cone effect and inclusive

jets can likely be attributed to the different Casimir factors of quarks and gluons, as the inclusive jet sample is a mixture of gluon- and light-quark-initiated jets.

6 Summary

In this paper, the measurement of the production yield and nuclear modification factor of charm jets tagged with fully reconstructed D⁰ mesons in central (0–10%) Pb–Pb collisions at a centre-of-mass energy per nucleon pair $\sqrt{s_{\text{NN}}} = 5.02 \text{ TeV}$ has been reported. The use of D⁰ mesons for charm-jet tagging extends the measurement of the charm-jet production to transverse momentum values down to $p_T^{\text{ch jet}} = 5 \text{ GeV}/c$.

The nuclear modification factor of charm jets tagged with D⁰ mesons, which quantifies the suppression of the jet yield due to interactions with the medium, was measured for the first time. It was computed by comparing the D⁰-jet yield in Pb–Pb collisions with the production cross section of D⁰-tagged jets in pp collisions at the same collision energy as a reference and it was found to be suppressed in the full measured p_T range. The comparison with the nuclear modification factor of inclusive jets at the same centre-of-mass energy and centrality class indicates a lower suppression of charm jets compared to light-quark and gluon jets when traversing the medium, with a significance of about 2σ in the transverse momentum range $20 < p_T^{\text{ch jet}} < 50 \text{ GeV}/c$. This difference can be attributed to the interplay of effects arising from the mass of the initial quark and the colour charge. The heavier quark mass suppresses the energy loss of charm quarks compared to light quarks, while the larger colour charge enhances the energy loss for gluon-initiated jets, which are more abundant at lower p_T , compared to quark-initiated jets.

The results are compared with JETSCAPE, Dai et al., and LIDO theoretical calculations of in-medium energy loss including quark-mass and colour-charge effects. Among the models considered, LIDO qualitatively describes the ordering between charm jets and inclusive jets and it also shows the best quantitative agreement with the data. Specific modifications of the LIDO predictions indicate that dead-cone effect is an important factor in the suppression of radiative processes and it is a fundamental factor differentiating the nuclear modification factor of inclusive jets from that of D⁰-tagged jets in the kinematic region of the measurement.

A difference is found in the LIDO model also between the R_{AA} of inclusive jets and that of charm jets without dead-cone effect and it can be attributed to the influence of colour charge effects. The other theoretical predictions tend to underestimate the nuclear modification factor of charm jets.

Overall, this measurement provides important insights into the modification of charm jets in the QGP created in heavy-ion collisions and sheds light on the quark-mass and colour-charge dependence of the in-medium energy loss mechanisms.

Acknowledgements

The ALICE Collaboration would like to thank all its engineers and technicians for their invaluable contributions to the construction of the experiment and the CERN accelerator teams for the outstanding performance of the LHC complex. The ALICE Collaboration gratefully acknowledges the resources and support provided by all Grid centres and the Worldwide LHC Computing Grid (WLCG) collaboration. The ALICE Collaboration acknowledges the following funding agencies for their support in building and running the ALICE detector: A. I. Alikhanyan National Science Laboratory (Yerevan Physics Institute) Foundation (ANSL), State Committee of Science and World Federation of Scientists (WFS), Armenia; Austrian Academy of Sciences, Austrian Science Fund (FWF): [M 2467-N36] and Nationalstiftung für Forschung, Technologie und Entwicklung, Austria; Ministry of Communications and High Technologies, National Nuclear Research Center, Azerbaijan; Conselho Nacional de Desenvolvimento

Científico e Tecnológico (CNPq), Financiadora de Estudos e Projetos (Finep), Fundação de Amparo à Pesquisa do Estado de São Paulo (FAPESP) and Universidade Federal do Rio Grande do Sul (UFRGS), Brazil; Bulgarian Ministry of Education and Science, within the National Roadmap for Research Infrastructures 2020-2027 (object CERN), Bulgaria; Ministry of Education of China (MOEC) , Ministry of Science & Technology of China (MSTC) and National Natural Science Foundation of China (NSFC), China; Ministry of Science and Education and Croatian Science Foundation, Croatia; Centro de Aplicaciones Tecnológicas y Desarrollo Nuclear (CEADEN), Cubaenergía, Cuba; Ministry of Education, Youth and Sports of the Czech Republic, Czech Republic; The Danish Council for Independent Research | Natural Sciences, the VILLUM FONDEN and Danish National Research Foundation (DNRF), Denmark; Helsinki Institute of Physics (HIP), Finland; Commissariat à l'Energie Atomique (CEA) and Institut National de Physique Nucléaire et de Physique des Particules (IN2P3) and Centre National de la Recherche Scientifique (CNRS), France; Bundesministerium für Bildung und Forschung (BMBF) and GSI Helmholtzzentrum für Schwerionenforschung GmbH, Germany; General Secretariat for Research and Technology, Ministry of Education, Research and Religions, Greece; National Research, Development and Innovation Office, Hungary; Department of Atomic Energy Government of India (DAE), Department of Science and Technology, Government of India (DST), University Grants Commission, Government of India (UGC) and Council of Scientific and Industrial Research (CSIR), India; National Research and Innovation Agency - BRIN, Indonesia; Istituto Nazionale di Fisica Nucleare (INFN), Italy; Japanese Ministry of Education, Culture, Sports, Science and Technology (MEXT) and Japan Society for the Promotion of Science (JSPS) KAKENHI, Japan; Consejo Nacional de Ciencia (CONACYT) y Tecnología, through Fondo de Cooperación Internacional en Ciencia y Tecnología (FONCICYT) and Dirección General de Asuntos del Personal Académico (DGAPA), Mexico; Nederlandse Organisatie voor Wetenschappelijk Onderzoek (NWO), Netherlands; The Research Council of Norway, Norway; Pontificia Universidad Católica del Perú, Peru; Ministry of Science and Higher Education, National Science Centre and WUT ID-UB, Poland; Korea Institute of Science and Technology Information and National Research Foundation of Korea (NRF), Republic of Korea; Ministry of Education and Scientific Research, Institute of Atomic Physics, Ministry of Research and Innovation and Institute of Atomic Physics and Universitatea Națională de Știință și Tehnologie Politehnica București, Romania; Ministry of Education, Science, Research and Sport of the Slovak Republic, Slovakia; National Research Foundation of South Africa, South Africa; Swedish Research Council (VR) and Knut & Alice Wallenberg Foundation (KAW), Sweden; European Organization for Nuclear Research, Switzerland; Suranaree University of Technology (SUT), National Science and Technology Development Agency (NSTDA) and National Science, Research and Innovation Fund (NSRF via PMU-B B05F650021), Thailand; Turkish Energy, Nuclear and Mineral Research Agency (TENMAK), Turkey; National Academy of Sciences of Ukraine, Ukraine; Science and Technology Facilities Council (STFC), United Kingdom; National Science Foundation of the United States of America (NSF) and United States Department of Energy, Office of Nuclear Physics (DOE NP), United States of America. In addition, individual groups or members have received support from: Czech Science Foundation (grant no. 23-07499S), Czech Republic; FORTE project, reg. no. CZ.02.01.01/00/22_008/0004632, Czech Republic, co-funded by the European Union, Czech Republic; European Research Council (grant no. 950692), European Union; ICSC - Centro Nazionale di Ricerca in High Performance Computing, Big Data and Quantum Computing, European Union - NextGenerationEU; Academy of Finland (Center of Excellence in Quark Matter) (grant nos. 346327, 346328), Finland.

References

- [1] U. W. Heinz and M. Jacob, “Evidence for a new state of matter: An Assessment of the results from the CERN lead beam program”, arXiv:nucl-th/0002042.
- [2] W. Busza, K. Rajagopal, and W. van der Schee, “Heavy Ion Collisions: The Big Picture, and the Big Questions”, *Ann. Rev. Nucl. Part. Sci.* **68** (2018) 339–376, arXiv:1802.04801 [hep-ph].

- [3] ALICE Collaboration, S. Acharya *et al.*, “The ALICE experiment: a journey through QCD”, *Eur. Phys. J. C* **84** (2024) 813, arXiv:2211.04384 [nucl-ex].
- [4] HotQCD Collaboration, A. Bazavov *et al.*, “Chiral crossover in QCD at zero and non-zero chemical potentials”, *Phys. Lett. B* **795** (2019) 15–21, arXiv:1812.08235 [hep-lat].
- [5] S. Borsanyi *et al.*, “QCD Crossover at Finite Chemical Potential from Lattice Simulations”, *Phys. Rev. Lett.* **125** (2020) 052001, arXiv:2002.02821 [hep-lat].
- [6] H. Satz, “Colour deconfinement and quarkonium binding”, *J. Phys. G* **32** (2006) R25, arXiv:hep-ph/0512217.
- [7] STAR Collaboration, J. Adams *et al.*, “Experimental and theoretical challenges in the search for the quark gluon plasma: The STAR Collaboration’s critical assessment of the evidence from RHIC collisions”, *Nucl. Phys. A* **757** (2005) 102–183, arXiv:nucl-ex/0501009.
- [8] STAR Collaboration, J. Adams *et al.*, “Direct observation of dijets in central Au+Au collisions at $\sqrt{s_{\text{NN}}} = 200 \text{ GeV}$ ”, *Phys. Rev. Lett.* **97** (2006) 162301, arXiv:nucl-ex/0604018.
- [9] PHENIX Collaboration, S. S. Adler *et al.*, “Dense-Medium Modifications to Jet-Induced Hadron Pair Distributions in Au+Au Collisions at $\sqrt{s_{\text{NN}}} = 200 \text{ GeV}$ ”, *Phys. Rev. Lett.* **97** (2006) 052301, arXiv:nucl-ex/0507004.
- [10] STAR Collaboration, C. Adler *et al.*, “Centrality dependence of high p_T hadron suppression in Au+Au collisions at $\sqrt{s_{\text{NN}}} = 130 \text{ GeV}$ ”, *Phys. Rev. Lett.* **89** (2002) 202301, arXiv:nucl-ex/0206011.
- [11] PHENIX Collaboration, K. Adcox *et al.*, “Formation of dense partonic matter in relativistic nucleus-nucleus collisions at RHIC: Experimental evaluation by the PHENIX collaboration”, *Nucl. Phys. A* **757** (2005) 184–283, arXiv:nucl-ex/0410003.
- [12] F.-M. Liu and S.-X. Liu, “QGP formation time and direct photons from heavy ion collisions”, *Phys. Rev. C* **89** (2014) 034906, arXiv:1212.6587 [nucl-th].
- [13] A. Andronic *et al.*, “Heavy-flavour and quarkonium production in the LHC era: from proton–proton to heavy-ion collisions”, *Eur. Phys. J. C* **76** (2016) 107, arXiv:1506.03981 [nucl-ex].
- [14] M. Djordjevic, “Heavy flavor puzzle at LHC: a serendipitous interplay of jet suppression and fragmentation”, *Phys. Rev. Lett.* **112** (2014) 042302, arXiv:1307.4702 [nucl-th].
- [15] Particle Data Group Collaboration, M. Tanabashi *et al.*, “Review of Particle Physics”, *Phys. Rev. D* **98** (2018) 030001.
- [16] A. Buckley *et al.*, “General-purpose event generators for LHC physics”, *Phys. Rept.* **504** (2011) 145–233, arXiv:1101.2599 [hep-ph].
- [17] I. M. Dremin and J. W. Gary, “Hadron multiplicities”, *Phys. Rept.* **349** (2001) 301–393, arXiv:hep-ph/0004215.
- [18] ALICE Collaboration, S. Acharya *et al.*, “Direct observation of the dead-cone effect in quantum chromodynamics”, *Nature* **605** (2022) 440–446, arXiv:2106.05713 [nucl-ex]. [Erratum: *Nature* 607, E22 (2022)].
- [19] J. Aichelin, P. B. Gossiaux, and T. Gousset, “Radiative and Collisional Energy Loss of Heavy Quarks in Deconfined Matter”, *Acta Phys. Polon. B* **43** (2012) 655–662, arXiv:1201.4192 [nucl-th].

- [20] N. Armesto, C. A. Salgado, and U. A. Wiedemann, “Medium induced gluon radiation off massive quarks fills the dead cone”, *Phys. Rev. D* **69** (2004) 114003, arXiv:hep-ph/0312106.
- [21] B.-W. Zhang, E. Wang, and X.-N. Wang, “Heavy quark energy loss in nuclear medium”, *Phys. Rev. Lett.* **93** (2004) 072301, arXiv:nucl-th/0309040.
- [22] M. Djordjevic and M. Gyulassy, “Heavy quark radiative energy loss in QCD matter”, *Nucl. Phys. A* **733** (2004) 265–298, arXiv:nucl-th/0310076.
- [23] M. L. Miller, K. Reygers, S. J. Sanders, and P. Steinberg, “Glauber modeling in high energy nuclear collisions”, *Ann. Rev. Nucl. Part. Sci.* **57** (2007) 205–243, arXiv:nucl-ex/0701025.
- [24] D. d’Enterria and C. Loizides, “Progress in the Glauber Model at Collider Energies”, *Ann. Rev. Nucl. Part. Sci.* **71** (2021) 315–344, arXiv:2011.14909 [hep-ph].
- [25] ALICE Collaboration, S. Acharya *et al.*, “Measurement of D^0 , D^+ , D^{*+} and D_s^+ production in Pb–Pb collisions at $\sqrt{s_{\text{NN}}} = 5.02$ TeV”, *JHEP* **10** (2018) 174, arXiv:1804.09083 [nucl-ex].
- [26] ALICE Collaboration, J. Adam *et al.*, “Centrality dependence of high- p_T D meson suppression in Pb–Pb collisions at $\sqrt{s_{\text{NN}}} = 2.76$ TeV”, *JHEP* **11** (2015) 205, arXiv:1506.06604 [nucl-ex]. [Addendum: JHEP 06, 32 (2017)].
- [27] ALICE Collaboration, S. Acharya *et al.*, “Measurement of beauty production via non-prompt D^0 mesons in Pb–Pb collisions at $\sqrt{s_{\text{NN}}} = 5.02$ TeV”, *JHEP* **12** (2022) 126, arXiv:2202.00815 [nucl-ex].
- [28] ALICE Collaboration, S. Acharya *et al.*, “Centrality and transverse momentum dependence of inclusive J/ψ production at midrapidity in Pb–Pb collisions at $\sqrt{s} = 5.02$ TeV”, *Phys. Lett. B* **805** (2020) 135434, arXiv:1910.14404 [nucl-ex].
- [29] CMS Collaboration, A. M. Sirunyan *et al.*, “Nuclear modification factor of D^0 mesons in PbPb collisions at $\sqrt{s_{\text{NN}}} = 5.02$ TeV”, *Phys. Lett. B* **782** (2018) 474–496, arXiv:1708.04962.
- [30] CMS Collaboration, S. Chatrchyan *et al.*, “Observation of sequential Υ suppression in PbPb collisions”, *Phys. Rev. Lett.* **109** (2012) 222301, arXiv:1208.2826. [Erratum: *Phys. Rev. Lett.* **120**, 199903 (2018)].
- [31] CMS Collaboration, S. Chatrchyan *et al.*, “Suppression of non-prompt J/ψ , prompt J/ψ , and $\Upsilon(1S)$ in PbPb collisions at $\sqrt{s_{\text{NN}}} = 2.76$ TeV”, *JHEP* **2012** (2012) 063, arXiv:1201.5069.
- [32] ATLAS Collaboration, M. Aaboud *et al.*, “Measurement of the suppression and azimuthal anisotropy of muons from heavy-flavor decays in Pb+Pb collisions at $\sqrt{s_{\text{NN}}} = 2.76$ TeV with the ATLAS detector”, *Phys. Rev. C* **98** (2018) 044905, arXiv:1805.05220 [nucl-ex].
- [33] ATLAS Collaboration, G. Aad *et al.*, “Measurement of the nuclear modification factor for muons from charm and bottom hadrons in Pb+Pb collisions at 5.02 TeV with the ATLAS detector”, *Phys. Lett. B* **829** (2022) 137077, arXiv:2109.00411.
- [34] ATLAS Collaboration, M. Aaboud *et al.*, “Prompt and non-prompt J/ψ and $\psi(2S)$ suppression at high transverse momentum in $\sqrt{s_{\text{NN}}} = 5.02$ TeV Pb+Pb collisions with the ATLAS experiment”, *Eur. Phys. J. C* **78** 762, arXiv:1805.04077 [nucl-ex].
- [35] ALICE Collaboration, S. Acharya *et al.*, “Measurement of electrons from beauty-hadron decays in pp and Pb–Pb collisions at $\sqrt{s_{\text{NN}}} = 5.02$ TeV”, *Phys. Rev. C* **108** (2023) 034906, arXiv:2211.13985 [nucl-ex].

- [36] CMS Collaboration, A. M. Sirunyan *et al.*, “Measurement of the B^\pm Meson Nuclear Modification Factor in Pb-Pb Collisions at $\sqrt{s_{NN}} = 5.02$ TeV”, *Phys. Rev. Lett.* **119** (2017) 152301, arXiv:1705.04727 [hep-ex].
- [37] ALICE Collaboration, S. Acharya *et al.*, “Measurement of beauty-strange meson production in Pb-Pb collisions at $\sqrt{s_{NN}} = 5.02$ TeV via non-prompt D_s^+ mesons”, *Phys. Lett. B* **846** (2023) 137561, arXiv:2204.10386 [nucl-ex].
- [38] CMS Collaboration, A. M. Sirunyan *et al.*, “Measurement of prompt and nonprompt charmonium suppression in PbPb collisions at 5.02 TeV”, *Eur. Phys. J. C* **78** (2018) 509, arXiv:1712.08959 [nucl-ex]. [Erratum: Eur.Phys.J.C 83, 145 (2023)].
- [39] CMS Collaboration, A. M. Sirunyan *et al.*, “Studies of charm quark diffusion inside jets using PbPb and pp collisions at $\sqrt{s_{NN}} = 5.02$ TeV”, *Phys. Rev. Lett.* **125** (2020) 102001, arXiv:1911.01461 [hep-ex].
- [40] ATLAS Collaboration, G. Aad *et al.*, “Measurement of the nuclear modification factor of b -jets in 5.02 TeV Pb+Pb collisions with the ATLAS detector”, *Eur. Phys. J. C* **83** (2023) 438, arXiv:2204.13530 [nucl-ex].
- [41] ATLAS Collaboration, G. Aad *et al.*, “Comparison of inclusive and photon-tagged jet suppression in 5.02 TeV Pb+Pb collisions with ATLAS”, *Phys. Lett. B* **846** (2023) 138154, arXiv:2303.10090 [nucl-ex].
- [42] ALICE Collaboration, K. Aamodt *et al.*, “The ALICE experiment at the CERN LHC”, *JINST* **3** (2008) S08002.
- [43] ALICE Collaboration, K. Aamodt *et al.*, “Alignment of the ALICE Inner Tracking System with cosmic-ray tracks”, *JINST* **5** (2010) P03003, arXiv:1001.0502 [physics.ins-det].
- [44] J. Alme *et al.*, “The ALICE TPC, a large 3-dimensional tracking device with fast readout for ultra-high multiplicity events”, *Nucl. Instrum. Meth. A* **622** (2010) 316–367, arXiv:1001.1950 [physics.ins-det].
- [45] A. Akindinov *et al.*, “Performance of the ALICE Time-Of-Flight detector at the LHC”, *Eur. Phys. J. Plus* **128** (2013) 44.
- [46] ALICE Collaboration, E. Abbas *et al.*, “Performance of the ALICE VZERO system”, *JINST* **8** (2013) P10016, arXiv:1306.3130 [nucl-ex].
- [47] G. Puddu *et al.*, “The zero degree calorimeters for the ALICE experiment”, *Nucl. Instrum. Meth. A* **581** (2007) 397–401. [Erratum: Nucl.Instrum.Meth.A 604, 765 (2009)].
- [48] ALICE Collaboration, J. Adam *et al.*, “Centrality dependence of the charged-particle multiplicity density at midrapidity in Pb-Pb collisions at $\sqrt{s_{NN}} = 5.02$ TeV”, *Phys. Rev. Lett.* **116** (2016) 222302, arXiv:1512.06104 [nucl-ex].
- [49] ALICE Collaboration, “Centrality determination in heavy ion collisions”, ALICE-PUBLIC-2018-011 (2018). <https://cds.cern.ch/record/2636623>.
- [50] ALICE Collaboration, S. Acharya *et al.*, “Measurement of the production of charm jets tagged with D^0 mesons in pp collisions at $\sqrt{s} = 5.02$ and 13 TeV”, *JHEP* **06** (2023) 133, arXiv:2204.10167 [nucl-ex].
- [51] T. Sjostrand, S. Mrenna, and P. Z. Skands, “A Brief Introduction to PYTHIA 8.1”, *Comput. Phys. Commun.* **178** (2008) 852–867, arXiv:0710.3820 [hep-ph].

- [52] P. Skands, S. Carrazza, and J. Rojo, “Tuning PYTHIA 8.1: the Monash 2013 Tune”, *Eur. Phys. J. C* **74** (2014) 3024, arXiv:1404.5630 [hep-ph].
- [53] ALICE Collaboration, B. Abelev *et al.*, “Pseudorapidity density of charged particles in p–Pb collisions at $\sqrt{s_{\text{NN}}} = 5.02 \text{ TeV}$ ”, *Phys. Rev. Lett.* **110** (2013) 032301, arXiv:1210.3615 [nucl-ex].
- [54] X.-N. Wang and M. Gyulassy, “HIJING: A Monte Carlo model for multiple jet production in pp, pA, and AA collisions”, *Phys. Rev. D* **44** (1991) 3501–3516.
- [55] R. Brun *et al.*, *GEANT: Detector Description and Simulation Tool; Oct 1994*. CERN Program Library. CERN, Geneva, 1993. <https://cds.cern.ch/record/1082634>. Long Writeup W5013.
- [56] ALICE Collaboration, S. Acharya *et al.*, “Prompt D⁰, D⁺, and D^{*+} production in Pb–Pb collisions at $\sqrt{s_{\text{NN}}} = 5.02 \text{ TeV}$ ”, *JHEP* **01** (2022) 174, arXiv:2110.09420 [nucl-ex].
- [57] M. Cacciari, G. P. Salam, and G. Soyez, “FastJet user manual”, *Eur. Phys. J. C* **72** (2012) 1896, arXiv:1111.6097 [hep-ph].
- [58] M. Cacciari, G. P. Salam, and G. Soyez, “The anti- k_t jet clustering algorithm”, *JHEP* **04** (2008) 063, arXiv:0802.1189 [hep-ph].
- [59] G. P. Salam, “Towards Jetography”, *Eur. Phys. J. C* **67** (2010) 637–686, arXiv:0906.1833 [hep-ph].
- [60] ALICE Collaboration, B. Abelev *et al.*, “Measurement of event background fluctuations for charged particle jet reconstruction in Pb–Pb collisions at $\sqrt{s_{\text{NN}}} = 2.76 \text{ TeV}$ ”, *JHEP* **03** (2012) 053, arXiv:1201.2423 [hep-ex].
- [61] ALICE Collaboration, B. Abelev *et al.*, “Measurement of charged jet suppression in Pb–Pb collisions at $\sqrt{s_{\text{NN}}} = 2.76 \text{ TeV}$ ”, *JHEP* **03** (2014) 013, arXiv:1311.0633 [nucl-ex].
- [62] ALICE Collaboration, J. Adam *et al.*, “Measurement of jet suppression in central Pb–Pb collisions at $\sqrt{s_{\text{NN}}} = 2.76 \text{ TeV}$ ”, *Phys. Lett. B* **746** (2015) 1–14, arXiv:1502.01689 [nucl-ex].
- [63] S. D. Ellis and D. E. Soper, “Successive combination jet algorithm for hadron collisions”, *Phys. Rev. D* **48** (1993) 3160–3166, arXiv:hep-ph/9305266.
- [64] ALICE Collaboration, S. Acharya *et al.*, “Measurement of D⁰, D⁺, D^{*+}, and D_s⁺ production in pp collisions at $\sqrt{s} = 5.02 \text{ TeV}$ with ALICE”, *Eur. Phys. J. C* **79** (2019) 388, arXiv:1901.07979 [nucl-ex].
- [65] ALICE Collaboration, S. Acharya *et al.*, “Measurement of the production of charm jets tagged with D⁰ mesons in pp collisions at $\sqrt{s} = 7 \text{ TeV}$ ”, *JHEP* **08** (2019) 133, arXiv:1905.02510 [nucl-ex].
- [66] P. Nason, “A New method for combining NLO QCD with shower Monte Carlo algorithms”, *JHEP* **11** (2004) 040, arXiv:hep-ph/0409146.
- [67] S. Frixione, P. Nason, and C. Oleari, “Matching NLO QCD computations with Parton Shower simulations: the POWHEG method”, *JHEP* **11** (2007) 070, arXiv:0709.2092 [hep-ph].
- [68] S. Alioli, P. Nason, C. Oleari, and E. Re, “A general framework for implementing NLO calculations in shower Monte Carlo programs: the POWHEG BOX”, *JHEP* **06** (2010) 043, arXiv:1002.2581 [hep-ph].

- [69] S. Alioli, K. Hamilton, P. Nason, C. Oleari, and E. Re, “Jet pair production in POWHEG”, *JHEP* **04** (2011) 081, arXiv:1012.3380 [hep-ph].
- [70] T. Sjostrand, S. Mrenna, and P. Z. Skands, “PYTHIA 6.4 Physics and Manual”, *JHEP* **05** (2006) 026, arXiv:hep-ph/0603175.
- [71] H.-L. Lai, M. Guzzi, J. Huston, Z. Li, P. M. Nadolsky, J. Pumplin, and C. P. Yuan, “New parton distributions for collider physics”, *Phys. Rev. D* **82** (2010) 074024, arXiv:1007.2241 [hep-ph].
- [72] A. Buckley *et al.*, “LHAPDF6: parton density access in the LHC precision era”, *Eur. Phys. J. C* **75** (2015) 132, arXiv:1412.7420 [hep-ph].
- [73] G. D’Agostini, “Improved iterative Bayesian unfolding”, in *Alliance Workshop on Unfolding and Data Correction*. 10, 2010. arXiv:1010.0632 [physics.data-an].
- [74] L. Brenner *et al.*, “Comparison of unfolding methods using rooFitunfold”, *International Journal of Modern Physics A* **35** (2020) 2050145, arXiv:1910.14654.
- [75] M. Cacciari, S. Frixione, N. Houdeau, M. L. Mangano, P. Nason, and G. Ridolfi, “Theoretical predictions for charm and bottom production at the LHC”, *JHEP* **10** (2012) 137, arXiv:1205.6344 [hep-ph].
- [76] ALICE Collaboration, S. Acharya *et al.*, “Measurements of inclusive jet spectra in pp and central Pb–Pb collisions at $\sqrt{s_{\text{NN}}} = 5.02 \text{ TeV}$ ”, *Phys. Rev. C* **101** (2020) 034911, arXiv:1909.09718 [nucl-ex].
- [77] ALICE Collaboration, S. Acharya *et al.*, “Measurement of the radius dependence of charged-particle jet suppression in Pb–Pb collisions at $\sqrt{s_{\text{NN}}} = 5.02 \text{ TeV}$ ”, *Phys. Lett. B* **849** (2024) 138412, arXiv:2303.00592 [nucl-ex].
- [78] ALICE Collaboration, S. Acharya *et al.*, “Measurement of charged jet cross section in pp collisions at $\sqrt{s} = 5.02 \text{ TeV}$ ”, *Phys. Rev. D* **100** (2019) 092004, arXiv:1905.02536 [nucl-ex].
- [79] J. H. Putschke *et al.*, “The JETSCAPE framework”, arXiv:1903.07706 [nucl-th].
- [80] W. Dai, S. Wang, S.-L. Zhang, B.-W. Zhang, and E. Wang, “Transverse Momentum Balance and Angular Distribution of $b\bar{b}$ Dijets in Pb+Pb collisions”, *Chin. Phys. C* **44** (2020) 104105, arXiv:1806.06332 [nucl-th].
- [81] W. Ke, Y. Xu, and S. A. Bass, “Modified Boltzmann approach for modeling the splitting vertices induced by the hot QCD medium in the deep Landau–Pomeranchuk–Migdal region”, *Phys. Rev. C* **100** (2019) 064911, arXiv:1810.08177 [nucl-th].
- [82] W. Ke, Y. Xu, and S. A. Bass, “Linearized Boltzmann–Langevin model for heavy quark transport in hot and dense QCD matter”, *Phys. Rev. C* **98** (2018) 064901, arXiv:1806.08848 [nucl-th].
- [83] S. Cao and A. Majumder, “Nuclear modification of leading hadrons and jets within a virtuality ordered parton shower”, *Phys. Rev. C* **101** (2020) 024903, arXiv:1712.10055 [nucl-th].
- [84] Y. He, T. Luo, X.-N. Wang, and Y. Zhu, “Linear Boltzmann Transport for Jet Propagation in the Quark-Gluon Plasma: Elastic Processes and Medium Recoil”, *Phys. Rev. C* **91** (2015) 054908, arXiv:1503.03313 [nucl-th]. [Erratum: *Phys. Rev. C* 97, 019902 (2018)].
- [85] W. Ke and X.-N. Wang, “QGP modification to single inclusive jets in a calibrated transport model”, *JHEP* **05** (2021) 041, arXiv:2010.13680 [hep-ph].

A The ALICE Collaboration

S. Acharya ¹²⁷, A. Agarwal¹³⁵, G. Aglieri Rinella ³², L. Aglietta ²⁴, M. Agnello ²⁹, N. Agrawal ²⁵, Z. Ahammed ¹³⁵, S. Ahmad ¹⁵, S.U. Ahn ⁷¹, I. Ahuja ³⁷, A. Akindinov ¹⁴⁰, V. Akishina³⁸, M. Al-Turany ⁹⁷, D. Aleksandrov ¹⁴⁰, B. Alessandro ⁵⁶, H.M. Alfanda ⁶, R. Alfaro Molina ⁶⁷, B. Ali ¹⁵, A. Alici ²⁵, N. Alizadehvandchali ¹¹⁶, A. Alkin ¹⁰⁴, J. Alme ²⁰, G. Alocco ^{24,52}, T. Alt ⁶⁴, A.R. Altamura ⁵⁰, I. Altsybeev ⁹⁵, J.R. Alvarado ⁴⁴, C.O.R. Alvarez⁴⁴, M.N. Anaam ⁶, C. Andrei ⁴⁵, N. Andreou ¹¹⁵, A. Andronic ¹²⁶, E. Andronov ¹⁴⁰, V. Anguelov ⁹⁴, F. Antinori ⁵⁴, P. Antonioli ⁵¹, N. Apadula ⁷⁴, L. Aphecetche ¹⁰³, H. Appelshäuser ⁶⁴, C. Arata ⁷³, S. Arcelli ²⁵, R. Arnaldi ⁵⁶, J.G.M.C.A. Arneiro ¹¹⁰, I.C. Arsene ¹⁹, M. Arslanbekov ¹³⁸, A. Augustinus ³², R. Averbeck ⁹⁷, D. Averyanov ¹⁴⁰, M.D. Azmi ¹⁵, H. Baba¹²⁴, A. Badalà ⁵³, J. Bae ¹⁰⁴, Y.W. Baek ⁴⁰, X. Bai ¹²⁰, R. Bailhache ⁶⁴, Y. Bailung ⁴⁸, R. Bala ⁹¹, A. Balbino ²⁹, A. Baldissari ¹³⁰, B. Balis ², Z. Banoo ⁹¹, V. Barbasova³⁷, F. Barile ³¹, L. Barioglio ⁵⁶, M. Barlou⁷⁸, B. Barman⁴¹, G.G. Barnaföldi ⁴⁶, L.S. Barnby ¹¹⁵, E. Barreau ¹⁰³, V. Barret ¹²⁷, L. Barreto ¹¹⁰, C. Bartels ¹¹⁹, K. Barth ³², E. Bartsch ⁶⁴, N. Bastid ¹²⁷, S. Basu ⁷⁵, G. Batigne ¹⁰³, D. Battistini ⁹⁵, B. Batyunya ¹⁴¹, D. Bauri⁴⁷, J.L. Bazo Alba ¹⁰¹, I.G. Bearden ⁸³, C. Beattie ¹³⁸, P. Becht ⁹⁷, D. Behera ⁴⁸, I. Belikov ¹²⁹, A.D.C. Bell Hechavarria ¹²⁶, F. Bellini ²⁵, R. Bellwied ¹¹⁶, S. Belokurova ¹⁴⁰, L.G.E. Beltran ¹⁰⁹, Y.A.V. Beltran ⁴⁴, G. Bencedi ⁴⁶, A. Bensaoula¹¹⁶, S. Beole ²⁴, Y. Berdnikov ¹⁴⁰, A. Berdnikova ⁹⁴, L. Bergmann ⁹⁴, M.G. Besoiu ⁶³, L. Betev ³², P.P. Bhaduri ¹³⁵, A. Bhasin ⁹¹, B. Bhattacharjee ⁴¹, L. Bianchi ²⁴, J. Bielčík ³⁵, J. Bielčíková ⁸⁶, A.P. Bigot ¹²⁹, A. Bilandzic ⁹⁵, G. Biro ⁴⁶, S. Biswas ⁴, N. Bize ¹⁰³, J.T. Blair ¹⁰⁸, D. Blau ¹⁴⁰, M.B. Blidaru ⁹⁷, N. Bluhme³⁸, C. Blume ⁶⁴, G. Boca ^{21,55}, F. Bock ⁸⁷, T. Bodova ²⁰, J. Bok ¹⁶, L. Boldizsár ⁴⁶, M. Bombara ³⁷, P.M. Bond ³², G. Bonomi ^{134,55}, H. Borel ¹³⁰, A. Borissov ¹⁴⁰, A.G. Borquez Carcamo ⁹⁴, E. Botta ²⁴, Y.E.M. Bouziani ⁶⁴, L. Bratrud ⁶⁴, P. Braun-Munzinger ⁹⁷, M. Bregant ¹¹⁰, M. Broz ³⁵, G.E. Bruno ^{96,31}, V.D. Buchakchiev ³⁶, M.D. Buckland ⁸⁵, D. Budnikov ¹⁴⁰, H. Buesching ⁶⁴, S. Bufalino ²⁹, P. Buhler ¹⁰², N. Burmasov ¹⁴⁰, Z. Buthelezi ^{68,123}, A. Bylinkin ²⁰, S.A. Bysiak¹⁰⁷, J.C. Cabanillas Noris ¹⁰⁹, M.F.T. Cabrera¹¹⁶, M. Cai ⁶, H. Caines ¹³⁸, A. Caliva ²⁸, E. Calvo Villar ¹⁰¹, J.M.M. Camacho ¹⁰⁹, P. Camerini ²³, F.D.M. Canedo ¹¹⁰, S.L. Cantway ¹³⁸, M. Carabas ¹¹³, A.A. Carballo ³², F. Carnesecchi ³², R. Caron ¹²⁸, L.A.D. Carvalho ¹¹⁰, J. Castillo Castellanos ¹³⁰, M. Castoldi ³², F. Catalano ³², S. Cattaruzzi ²³, C. Ceballos Sanchez ⁷, R. Cerri ²⁴, I. Chakaberia ⁷⁴, P. Chakraborty ¹³⁶, S. Chandra ¹³⁵, S. Chapelard ³², M. Chartier ¹¹⁹, S. Chattopadhyay¹³⁵, S. Chattopadhyay ¹³⁵, S. Chattpadhyay ⁹⁹, M. Chen³⁹, T. Cheng ⁶, C. Cheshkov ¹²⁸, V. Chibante Barroso ³², D.D. Chinellato ¹⁰², E.S. Chizzali ^{II,95}, J. Cho ⁵⁸, S. Cho ⁵⁸, P. Chochula ³², Z.A. Chochulska¹³⁶, D. Choudhury⁴¹, P. Christakoglou ⁸⁴, C.H. Christensen ⁸³, P. Christiansen ⁷⁵, T. Chujo ¹²⁵, M. Ciacco ²⁹, C. Cicalo ⁵², M.R. Ciupek⁹⁷, G. Clai^{III,51}, F. Colamaria ⁵⁰, J.S. Colburn¹⁰⁰, D. Colella ³¹, A. Colelli³¹, M. Colocci ²⁵, M. Concas ³², G. Conesa Balbastre ⁷³, Z. Conesa del Valle ¹³¹, G. Contin ²³, J.G. Contreras ³⁵, M.L. Coquet ¹⁰³, P. Cortese ^{133,56}, M.R. Cosentino ¹¹², F. Costa ³², S. Costanza ^{21,55}, C. Cot ¹³¹, P. Crochet ¹²⁷, R. Cruz-Torres ⁷⁴, M.M. Czarnynoga¹³⁶, A. Dainese ⁵⁴, G. Dange³⁸, M.C. Danisch ⁹⁴, A. Danu ⁶³, P. Das ⁸⁰, S. Das ⁴, A.R. Dash ¹²⁶, S. Dash ⁴⁷, A. De Caro ²⁸, G. de Cataldo ⁵⁰, J. de Cuveland³⁸, A. De Falco ²², D. De Gruttola ²⁸, N. De Marco ⁵⁶, C. De Martin ²³, S. De Pasquale ²⁸, R. Deb ¹³⁴, R. Del Grande ⁹⁵, L. Dello Stritto ³², W. Deng ⁶, K.C. Devereaux¹⁸, P. Dhankher ¹⁸, D. Di Bari ³¹, A. Di Mauro ³², B. Di Ruzza ¹³², B. Diab ¹³⁰, R.A. Diaz ^{141,7}, T. Dietel ¹¹⁴, Y. Ding ⁶, J. Ditzel ⁶⁴, R. Divià ³², Ø. Djupsland²⁰, U. Dmitrieva ¹⁴⁰, A. Dobrin ⁶³, B. Dönigus ⁶⁴, J.M. Dubinski ¹³⁶, A. Dubla ⁹⁷, P. Dupieux ¹²⁷, N. Dzalaiova¹³, T.M. Eder ¹²⁶, R.J. Ehlers ⁷⁴, F. Eisenhut ⁶⁴, R. Ejima ⁹², D. Elia ⁵⁰, B. Erasmus ¹⁰³, F. Ercolelli ²⁵, B. Espagnon ¹³¹, G. Eulisse ³², D. Evans ¹⁰⁰, S. Evdokimov ¹⁴⁰, L. Fabbietti ⁹⁵, M. Faggin ²³, J. Faivre ⁷³, F. Fan ⁶, W. Fan ⁷⁴, A. Fantoni ⁴⁹, M. Fasel ⁸⁷, A. Feliciello ⁵⁶, G. Feofilov ¹⁴⁰, A. Fernández Téllez ⁴⁴, L. Ferrandi ¹¹⁰, M.B. Ferrer ³², A. Ferrero ¹³⁰, C. Ferrero ^{IV,56}, A. Ferretti ²⁴, V.J.G. Feuillard ⁹⁴, V. Filova ³⁵, D. Finogeev ¹⁴⁰, F.M. Fionda ⁵², E. Flatland³², F. Flor ^{138,116}, A.N. Flores ¹⁰⁸, S. Foertsch ⁶⁸, I. Fokin ⁹⁴, S. Fokin ¹⁴⁰, U. Follo ^{IV,56}, E. Fragiocomo ⁵⁷, E. Frajna ⁴⁶, U. Fuchs ³², N. Funicello ²⁸, C. Furget ⁷³, A. Furs ¹⁴⁰, T. Fusayasu ⁹⁸, J.J. Gaardhøje ⁸³, M. Gagliardi ²⁴, A.M. Gago ¹⁰¹, T. Gahlaud ⁴⁷, C.D. Galvan ¹⁰⁹, S. Gami⁸⁰, D.R. Gangadharan ¹¹⁶, P. Ganoti ⁷⁸, C. Garabatos ⁹⁷, J.M. Garcia⁴⁴, T. García Chávez ⁴⁴, E. Garcia-Solis ⁹, C. Gargiulo ³², P. Gasik ⁹⁷, H.M. Gaur³⁸, A. Gautam ¹¹⁸, M.B. Gay Ducati ⁶⁶, M. Germain ¹⁰³, R.A. Gernhaeuser⁹⁵, C. Ghosh¹³⁵, M. Giacalone ⁵¹, G. Gioachin ²⁹, S.K. Giri¹³⁵, P. Giubellino ^{97,56}, P. Giubilato ²⁷, A.M.C. Glaenzer ¹³⁰, P. Glässel ⁹⁴, E. Glimos ¹²², D.J.Q. Goh⁷⁶, V. Gonzalez ¹³⁷, P. Gordeev ¹⁴⁰, M. Gorgon ², K. Goswami ⁴⁸, S. Gotovac ³³, V. Grabski ⁶⁷,

L.K. Graczykowski ¹³⁶, E. Grecka ⁸⁶, A. Grelli ⁵⁹, C. Grigoras ³², V. Grigoriev ¹⁴⁰, S. Grigoryan ^{141,1}, F. Grossa ³², J.F. Grosse-Oetringhaus ³², R. Grossi ⁹⁷, D. Grund ³⁵, N.A. Grunwald ⁹⁴, G.G. Guardiano ¹¹¹, R. Guernane ⁷³, M. Guilbaud ¹⁰³, K. Gulbrandsen ⁸³, J.J.W.K. Gumprecht ¹⁰², T. Gündem ⁶⁴, T. Gunji ¹²⁴, W. Guo ⁶, A. Gupta ⁹¹, R. Gupta ⁹¹, R. Gupta ⁴⁸, K. Gwizdziel ¹³⁶, L. Gyulai ⁴⁶, C. Hadjidakis ¹³¹, F.U. Haider ⁹¹, S. Haidlova ³⁵, M. Haldar ⁴, H. Hamagaki ⁷⁶, Y. Han ¹³⁹, B.G. Hanley ¹³⁷, R. Hannigan ¹⁰⁸, J. Hansen ⁷⁵, M.R. Haque ⁹⁷, J.W. Harris ¹³⁸, A. Harton ⁹, M.V. Hartung ⁶⁴, H. Hassan ¹¹⁷, D. Hatzifotiadou ⁵¹, P. Hauer ⁴², L.B. Havener ¹³⁸, E. Hellbär ³², H. Helstrup ³⁴, M. Hemmer ⁶⁴, T. Herman ³⁵, S.G. Hernandez ¹¹⁶, G. Herrera Corral ⁸, S. Herrmann ¹²⁸, K.F. Hetland ³⁴, B. Heybeck ⁶⁴, H. Hillemanns ³², B. Hippolyte ¹²⁹, I.P.M. Hobus ⁸⁴, F.W. Hoffmann ⁷⁰, B. Hofman ⁵⁹, G.H. Hong ¹³⁹, M. Horst ⁹⁵, A. Horzyk ², Y. Hou ⁶, P. Hristov ³², P. Huhn ⁶⁴, L.M. Huhta ¹¹⁷, T.J. Humanic ⁸⁸, A. Hutson ¹¹⁶, D. Hutter ³⁸, M.C. Hwang ¹⁸, R. Ilkaev ¹⁴⁰, M. Inaba ¹²⁵, G.M. Innocent ³², M. Ippolitov ¹⁴⁰, A. Isakov ⁸⁴, T. Isidori ¹¹⁸, M.S. Islam ⁹⁹, S. Iurchenko ¹⁴⁰, M. Ivanov ⁹⁷, M. Ivanov ¹³, V. Ivanov ¹⁴⁰, K.E. Iversen ⁷⁵, M. Jablonski ², B. Jacak ^{18,74}, N. Jacazio ²⁵, P.M. Jacobs ⁷⁴, S. Jadlovska ¹⁰⁶, J. Jadlovsky ¹⁰⁶, S. Jaelani ⁸², C. Jahnke ¹¹⁰, M.J. Jakubowska ¹³⁶, M.A. Janik ¹³⁶, T. Janson ⁷⁰, S. Ji ¹⁶, S. Jia ¹⁰, T. Jiang ¹⁰, A.A.P. Jimenez ⁶⁵, F. Jonas ⁷⁴, D.M. Jones ¹¹⁹, J.M. Jowett ^{32,97}, J. Jung ⁶⁴, M. Jung ⁶⁴, A. Junique ³², A. Jusko ¹⁰⁰, J. Kaewjai ¹⁰⁵, P. Kalinak ⁶⁰, A. Kalweit ³², A. Karasu Uysal ^{V,72}, D. Karatovic ⁸⁹, N. Karatzenis ¹⁰⁰, O. Karavichev ¹⁴⁰, T. Karavicheva ¹⁴⁰, E. Karpechev ¹⁴⁰, M.J. Karwowska ^{32,136}, U. Kebschull ⁷⁰, M. Keil ³², B. Ketzer ⁴², J. Keul ⁶⁴, S.S. Khade ⁴⁸, A.M. Khan ¹²⁰, S. Khan ¹⁵, A. Khanzadeev ¹⁴⁰, Y. Kharlov ¹⁴⁰, A. Khatun ¹¹⁸, A. Khuntia ³⁵, Z. Khuranova ⁶⁴, B. Kileng ³⁴, B. Kim ¹⁰⁴, C. Kim ¹⁶, D.J. Kim ¹¹⁷, E.J. Kim ⁶⁹, J. Kim ¹³⁹, J. Kim ⁵⁸, J. Kim ^{32,69}, M. Kim ¹⁸, S. Kim ¹⁷, T. Kim ¹³⁹, K. Kimura ⁹², A. Kirkova ³⁶, S. Kirsch ⁶⁴, I. Kisiel ³⁸, S. Kiselev ¹⁴⁰, A. Kisiel ¹³⁶, J.P. Kitowski ², J.L. Klay ⁵, J. Klein ³², S. Klein ⁷⁴, C. Klein-Bösing ¹²⁶, M. Kleiner ⁶⁴, T. Klemenz ⁹⁵, A. Kluge ³², C. Kobdaj ¹⁰⁵, R. Kohara ¹²⁴, T. Kollegger ⁹⁷, A. Kondratyev ¹⁴¹, N. Kondratyeva ¹⁴⁰, J. Konig ⁶⁴, S.A. Konigstorfer ⁹⁵, P.J. Konopka ³², G. Kornakov ¹³⁶, M. Korwieser ⁹⁵, S.D. Koryciak ², C. Koster ⁸⁴, A. Kotliarov ⁸⁶, N. Kovacic ⁸⁹, V. Kovalenko ¹⁴⁰, M. Kowalski ¹⁰⁷, V. Kozhuharov ³⁶, G. Kozlov ³⁸, I. Králik ⁶⁰, A. Kravčáková ³⁷, L. Krcal ^{32,38}, M. Krivda ^{100,60}, F. Krizek ⁸⁶, K. Krizkova Gajdosova ³², C. Krug ⁶⁶, M. Krüger ⁶⁴, D.M. Krupova ³⁵, E. Kryshen ¹⁴⁰, V. Kučera ⁵⁸, C. Kuhn ¹²⁹, P.G. Kuijer ⁸⁴, T. Kumaoka ¹²⁵, D. Kumar ¹³⁵, L. Kumar ⁹⁰, N. Kumar ⁹⁰, S. Kumar ⁵⁰, S. Kundu ³², P. Kurashvili ⁷⁹, A. Kurepin ¹⁴⁰, A.B. Kurepin ¹⁴⁰, A. Kuryakin ¹⁴⁰, S. Kushpil ⁸⁶, V. Kuskov ¹⁴⁰, M. Kutyla ¹³⁶, A. Kuznetsov ¹⁴¹, M.J. Kweon ⁵⁸, Y. Kwon ¹³⁹, S.L. La Pointe ³⁸, P. La Rocca ²⁶, A. Lakhathok ¹⁰⁵, M. Lamanna ³², A.R. Landou ⁷³, R. Langoy ¹²¹, P. Larionov ³², E. Laudi ³², L. Lautner ^{32,95}, R.A.N. Laveaga ¹⁰⁹, R. Lavicka ¹⁰², R. Lea ^{134,55}, H. Lee ¹⁰⁴, I. Legrand ⁴⁵, G. Legras ¹²⁶, J. Lehrbach ³⁸, A.M. Lejeune ³⁵, T.M. Lelek ², R.C. Lemmon ^{I,85}, I. León Monzón ¹⁰⁹, M.M. Lesch ⁹⁵, E.D. Lesser ¹⁸, P. Lévai ⁴⁶, M. Li ⁶, P. Li ¹⁰, X. Li ¹⁰, B.E. Liang-gilman ¹⁸, J. Lien ¹²¹, R. Lietava ¹⁰⁰, I. Likmeta ¹¹⁶, B. Lim ²⁴, S.H. Lim ¹⁶, V. Lindenstruth ³⁸, C. Lippmann ⁹⁷, D.H. Liu ⁶, J. Liu ¹¹⁹, G.S.S. Liveraro ¹¹¹, I.M. Lofnes ²⁰, C. Loizides ⁸⁷, S. Lokos ¹⁰⁷, J. Lömker ⁵⁹, X. Lopez ¹²⁷, E. López Torres ⁷, C. Lotteau ¹²⁸, P. Lu ^{97,120}, Z. Lu ¹⁰, F.V. Lugo ⁶⁷, J.R. Luhder ¹²⁶, M. Lunardon ²⁷, G. Luparello ⁵⁷, Y.G. Ma ³⁹, M. Mager ³², A. Maire ¹²⁹, E.M. Majerz ², M.V. Makarieva ³⁶, M. Malaev ¹⁴⁰, G. Malfattore ²⁵, N.M. Malik ⁹¹, S.K. Malik ⁹¹, L. Malinina ^{I,VIII,141}, D. Mallick ¹³¹, N. Mallick ⁴⁸, G. Mandaglio ^{30,53}, S.K. Mandal ⁷⁹, A. Manea ⁶³, V. Manko ¹⁴⁰, F. Manso ¹²⁷, V. Manzari ⁵⁰, Y. Mao ⁶, R.W. Marcjan ², G.V. Margagliotti ²³, A. Margotti ⁵¹, A. Marín ⁹⁷, C. Markert ¹⁰⁸, C.F.B. Marquez ³¹, P. Martinengo ³², M.I. Martínez ⁴⁴, G. Martínez García ¹⁰³, M.P.P. Martins ¹¹⁰, S. Masciocchi ⁹⁷, M. Masera ²⁴, A. Masoni ⁵², L. Massacrier ¹³¹, O. Massen ⁵⁹, A. Mastroserio ^{132,50}, O. Matonoha ⁷⁵, S. Mattiazzzo ²⁷, A. Matyja ¹⁰⁷, F. Mazzaschi ^{32,24}, M. Mazzilli ¹¹⁶, Y. Melikyan ⁴³, M. Melo ¹¹⁰, A. Menchaca-Rocha ⁶⁷, J.E.M. Mendez ⁶⁵, E. Meninno ¹⁰², A.S. Menon ¹¹⁶, M.W. Menzel ^{32,94}, M. Meres ¹³, Y. Miake ¹²⁵, L. Micheletti ³², D.L. Mihaylov ⁹⁵, K. Mikhaylov ^{141,140}, N. Minafra ¹¹⁸, D. Miškowiec ⁹⁷, A. Modak ¹³⁴, B. Mohanty ⁸⁰, M. Mohisin Khan ^{VI,15}, M.A. Molander ⁴³, S. Monira ¹³⁶, C. Mordasini ¹¹⁷, D.A. Moreira De Godoy ¹²⁶, I. Morozov ¹⁴⁰, A. Morsch ³², T. Mrnjavac ³², V. Muccifora ⁴⁹, S. Muhuri ¹³⁵, J.D. Mulligan ⁷⁴, A. Mulliri ²², M.G. Munhoz ¹¹⁰, R.H. Munzer ⁶⁴, H. Murakami ¹²⁴, S. Murray ¹¹⁴, L. Musa ³², J. Musinsky ⁶⁰, J.W. Myrcha ¹³⁶, B. Naik ¹²³, A.I. Nambrath ¹⁸, B.K. Nandi ⁴⁷, R. Nania ⁵¹, E. Nappi ⁵⁰, A.F. Nassirpour ¹⁷, A. Nath ⁹⁴, S. Nath ¹³⁵, C. Natrass ¹²², M.N. Naydenov ³⁶, A. Neagu ¹⁹, A. Negru ¹¹³, E. Nekrasova ¹⁴⁰, L. Nellen ⁶⁵, R. Nepeivoda ⁷⁵, S. Nese ¹⁹, N. Nicassio ⁵⁰, B.S. Nielsen ⁸³, E.G. Nielsen ⁸³, S. Nikolaev ¹⁴⁰, S. Nikulin ¹⁴⁰, V. Nikulin ¹⁴⁰, F. Noferini ⁵¹, S. Noh ¹², P. Nomokonov ¹⁴¹, J. Norman ¹¹⁹,

- N. Novitzky ⁸⁷, P. Nowakowski ¹³⁶, A. Nyanin ¹⁴⁰, J. Nystrand ²⁰, S. Oh ¹⁷, A. Ohlson ⁷⁵, V.A. Okorokov ¹⁴⁰, J. Oleniacz ¹³⁶, A.C. Oliveira Da Silva ¹²², A. Onnerstad ¹¹⁷, C. Oppedisano ⁵⁶, A. Ortiz Velasquez ⁶⁵, J. Otwinowski ¹⁰⁷, M. Oya ⁹², K. Oyama ⁷⁶, Y. Pachmayer ⁹⁴, S. Padhan ⁴⁷, D. Pagano ^{134,55}, G. Paić ⁶⁵, S. Paisano-Guzmán ⁴⁴, A. Palasciano ⁵⁰, I. Panasenko ⁷⁵, S. Panebianco ¹³⁰, C. Pantouvakis ²⁷, H. Park ¹²⁵, H. Park ¹⁰⁴, J. Park ¹²⁵, J.E. Parkkila ³², Y. Patley ⁴⁷, R.N. Patra ⁵⁰, B. Paul ¹³⁵, H. Pei ⁶, T. Peitzmann ⁵⁹, X. Peng ¹¹, M. Pennisi ²⁴, S. Perciballi ²⁴, D. Peresunko ¹⁴⁰, G.M. Perez ⁷, Y. Pestov ¹⁴⁰, M.T. Petersen ⁸³, V. Petrov ¹⁴⁰, M. Petrovici ⁴⁵, S. Piano ⁵⁷, M. Pikna ¹³, P. Pillot ¹⁰³, O. Pinazza ^{51,32}, L. Pinsky ¹¹⁶, C. Pinto ⁹⁵, S. Pisano ⁴⁹, M. Płoskoń ⁷⁴, M. Planinic ⁸⁹, F. Pliquet ⁶⁴, D.K. Plociennik ², M.G. Poghosyan ⁸⁷, B. Polichtchouk ¹⁴⁰, S. Politano ²⁹, N. Poljak ⁸⁹, A. Pop ⁴⁵, S. Porteboeuf-Houssais ¹²⁷, V. Pozdniakov ^{I,141}, I.Y. Pozos ⁴⁴, K.K. Pradhan ⁴⁸, S.K. Prasad ⁴, S. Prasad ⁴⁸, R. Preghenella ⁵¹, F. Prino ⁵⁶, C.A. Pruneau ¹³⁷, I. Pshenichnov ¹⁴⁰, M. Puccio ³², S. Pucillo ²⁴, S. Qiu ⁸⁴, L. Quaglia ²⁴, A.M.K. Radhakrishnan ⁴⁸, S. Ragoni ¹⁴, A. Rai ¹³⁸, A. Rakotozafindrabe ¹³⁰, L. Ramello ^{133,56}, F. Rami ¹²⁹, M. Rasa ²⁶, S.S. Räsänen ⁴³, R. Rath ⁵¹, M.P. Rauch ²⁰, I. Ravasenga ³², K.F. Read ^{87,122}, C. Reckziegel ¹¹², A.R. Redelbach ³⁸, K. Redlich ^{VII,79}, C.A. Reetz ⁹⁷, H.D. Regules-Medel ⁴⁴, A. Rehman ²⁰, F. Reidt ³², H.A. Reme-Ness ³⁴, K. Reygers ⁹⁴, A. Riabov ¹⁴⁰, V. Riabov ¹⁴⁰, R. Ricci ²⁸, M. Richter ²⁰, A.A. Riedel ⁹⁵, W. Riegler ³², A.G. Rifferto ²⁴, M. Rignanese ²⁷, C. Ripoli ²⁸, C. Ristea ⁶³, M.V. Rodriguez ³², M. Rodríguez Cahuantzi ⁴⁴, S.A. Rodríguez Ramírez ⁴⁴, K. Røed ¹⁹, R. Rogalev ¹⁴⁰, E. Rogochaya ¹⁴¹, T.S. Rogoschinski ⁶⁴, D. Rohr ³², D. Röhrich ²⁰, S. Rojas Torres ³⁵, P.S. Rokita ¹³⁶, G. Romanenko ²⁵, F. Ronchetti ³², E.D. Rosas ⁶⁵, K. Roslon ¹³⁶, A. Rossi ⁵⁴, A. Roy ⁴⁸, S. Roy ⁴⁷, N. Rubini ^{51,25}, J.A. Rudolph ⁸⁴, D. Ruggiano ¹³⁶, R. Rui ²³, P.G. Russek ², R. Russo ⁸⁴, A. Rustamov ⁸¹, E. Ryabinkin ¹⁴⁰, Y. Ryabov ¹⁴⁰, A. Rybicki ¹⁰⁷, J. Ryu ¹⁶, W. Rzesz ¹³⁶, B. Sabiu ⁵¹, S. Sadovsky ¹⁴⁰, J. Saetre ²⁰, K. Šafařík ³⁵, S. Saha ⁸⁰, B. Sahoo ⁴⁸, R. Sahoo ⁴⁸, S. Sahoo ⁶¹, D. Sahu ⁴⁸, P.K. Sahu ⁶¹, J. Saini ¹³⁵, K. Sajdakova ³⁷, S. Sakai ¹²⁵, M.P. Salvan ⁹⁷, S. Sambyal ⁹¹, D. Samitz ¹⁰², I. Sanna ^{32,95}, T.B. Saramela ¹¹⁰, D. Sarkar ⁸³, P. Sarma ⁴¹, V. Sarritzu ²², V.M. Sarti ⁹⁵, M.H.P. Sas ³², S. Sawan ⁸⁰, E. Scapparone ⁵¹, J. Schambach ⁸⁷, H.S. Scheid ⁶⁴, C. Schiaua ⁴⁵, R. Schicker ⁹⁴, F. Schlepper ⁹⁴, A. Schmah ⁹⁷, C. Schmidt ⁹⁷, H.R. Schmidt ⁹³, M.O. Schmidt ³², M. Schmidt ⁹³, N.V. Schmidt ⁸⁷, A.R. Schmier ¹²², R. Schotter ^{102,129}, A. Schröter ³⁸, J. Schukraft ³², K. Schweda ⁹⁷, G. Scioli ²⁵, E. Scomparin ⁵⁶, J.E. Seger ¹⁴, Y. Sekiguchi ¹²⁴, D. Sekihata ¹²⁴, M. Selina ⁸⁴, I. Selyuzhenkov ⁹⁷, S. Senyukov ¹²⁹, J.J. Seo ⁹⁴, D. Serebryakov ¹⁴⁰, L. Serkin ⁶⁵, L. Šerkšnytė ⁹⁵, A. Sevcenco ⁶³, T.J. Shaba ⁶⁸, A. Shabetai ¹⁰³, R. Shahoyan ³², A. Shangaraev ¹⁴⁰, B. Sharma ⁹¹, D. Sharma ⁴⁷, H. Sharma ⁵⁴, M. Sharma ⁹¹, S. Sharma ⁷⁶, S. Sharma ⁹¹, U. Sharma ⁹¹, A. Shatat ¹³¹, O. Sheibani ¹¹⁶, K. Shigaki ⁹², M. Shimomura ⁷⁷, J. Shin ¹², S. Shirinkin ¹⁴⁰, Q. Shou ³⁹, Y. Sibirski ¹⁴⁰, S. Siddhanta ⁵², T. Siemarczuk ⁷⁹, T.F. Silva ¹¹⁰, D. Silvermyr ⁷⁵, T. Simantathammakul ¹⁰⁵, R. Simeonov ³⁶, B. Singh ⁹¹, B. Singh ⁹⁵, K. Singh ⁴⁸, R. Singh ⁸⁰, R. Singh ⁹¹, R. Singh ⁹⁷, S. Singh ¹⁵, V.K. Singh ¹³⁵, V. Singhal ¹³⁵, T. Sinha ⁹⁹, B. Sitar ¹³, M. Sitta ^{133,56}, T.B. Skaali ¹⁹, G. Skorodumovs ⁹⁴, N. Smirnov ¹³⁸, R.J.M. Snellings ⁵⁹, E.H. Solheim ¹⁹, J. Song ¹⁶, C. Sonnabend ^{32,97}, J.M. Sonneveld ⁸⁴, F. Soramel ²⁷, A.B. Soto-hernandez ⁸⁸, R. Spijkers ⁸⁴, I. Sputowska ¹⁰⁷, J. Staa ⁷⁵, J. Stachel ⁹⁴, I. Stan ⁶³, P.J. Steffanic ¹²², T. Stellhorn ¹²⁶, S.F. Stiefelmaier ⁹⁴, D. Stocco ¹⁰³, I. Storehaug ¹⁹, N.J. Strangmann ⁶⁴, P. Stratmann ¹²⁶, S. Strazzi ²⁵, A. Sturniolo ^{30,53}, C.P. Stylianidis ⁸⁴, A.A.P. Suaside ¹¹⁰, C. Suire ¹³¹, M. Sukhanov ¹⁴⁰, M. Suljic ³², R. Sultanov ¹⁴⁰, V. Sumberia ⁹¹, S. Sumowidagdo ⁸², M. Szymkowski ¹³⁶, S.F. Taghavi ⁹⁵, G. Taillepied ⁹⁷, J. Takahashi ¹¹¹, G.J. Tambave ⁸⁰, S. Tang ⁶, Z. Tang ¹²⁰, J.D. Tapia Takaki ¹¹⁸, N. Tapus ¹¹³, L.A. Tarasovicova ³⁷, M.G. Tarzila ⁴⁵, G.F. Tassielli ³¹, A. Tauro ³², A. Tavira García ¹³¹, G. Tejeda Muñoz ⁴⁴, L. Terlizzi ²⁴, C. Terrevoli ⁵⁰, S. Thakur ⁴, D. Thomas ¹⁰⁸, A. Tikhonov ¹⁴⁰, N. Tiltmann ^{32,126}, A.R. Timmins ¹¹⁶, M. Tkacik ¹⁰⁶, T. Tkacik ¹⁰⁶, A. Toia ⁶⁴, R. Tokumoto ⁹², S. Tomassini ²⁵, K. Tomohiro ⁹², N. Topilskaya ¹⁴⁰, M. Toppi ⁴⁹, V.V. Torres ¹⁰³, A.G. Torres Ramos ³¹, A. Trifiró ^{30,53}, T. Triloki ⁹⁶, A.S. Triolo ^{32,30,53}, S. Tripathy ³², T. Tripathy ⁴⁷, S. Trogolo ²⁴, V. Trubnikov ³, W.H. Trzaska ¹¹⁷, T.P. Trzcinski ¹³⁶, C. Tsolanta ¹⁹, R. Tu ³⁹, A. Tumkin ¹⁴⁰, R. Turrisi ⁵⁴, T.S. Tveter ¹⁹, K. Ullaland ²⁰, B. Ulukutlu ⁹⁵, S. Upadhyaya ¹⁰⁷, A. Uras ¹²⁸, M. Urioni ¹³⁴, G.L. Usai ²², M. Vala ³⁷, N. Valle ⁵⁵, L.V.R. van Doremalen ⁵⁹, M. van Leeuwen ⁸⁴, C.A. van Veen ⁹⁴, R.J.G. van Weelden ⁸⁴, P. Vande Vyvre ³², D. Varga ⁴⁶, Z. Varga ⁴⁶, P. Vargas Torres ⁶⁵, M. Vasileiou ⁷⁸, A. Vasiliev ^{I,140}, O. Vázquez Doce ⁴⁹, O. Vazquez Rueda ¹¹⁶, V. Vechernin ¹⁴⁰, E. Vercellin ²⁴, S. Vergara Limón ⁴⁴, R. Verma ⁴⁷, L. Vermunt ⁹⁷, R. Vértesi ⁴⁶, M. Verweij ⁵⁹, L. Vickovic ³³, Z. Vilakazi ¹²³, O. Villalobos Baillie ¹⁰⁰, A. Villani ²³, A. Vinogradov ¹⁴⁰, T. Virgili ²⁸, M.M.O. Virta ¹¹⁷, A. Vodopyanov ¹⁴¹, B. Volkel ³², M.A. Völkl ⁹⁴, S.A. Voloshin ¹³⁷, G. Volpe ³¹, B. von Haller ³², I. Vorobyev ³², N. Vozniuk ¹⁴⁰,

J. Vrláková ³⁷, J. Wan³⁹, C. Wang ³⁹, D. Wang³⁹, Y. Wang ³⁹, Y. Wang ⁶, Z. Wang ³⁹, A. Wegrzynek ³², F.T. Weiglhofer³⁸, S.C. Wenzel ³², J.P. Wessels ¹²⁶, J. Wiechula ⁶⁴, J. Wikne ¹⁹, G. Wilk ⁷⁹, J. Wilkinson ⁹⁷, G.A. Willems ¹²⁶, B. Windelband ⁹⁴, M. Winn ¹³⁰, J.R. Wright ¹⁰⁸, W. Wu³⁹, Y. Wu ¹²⁰, Z. Xiong¹²⁰, R. Xu ⁶, A. Yadav ⁴², A.K. Yadav ¹³⁵, Y. Yamaguchi ⁹², S. Yang²⁰, S. Yano ⁹², E.R. Yeats¹⁸, Z. Yin ⁶, I.-K. Yoo ¹⁶, J.H. Yoon ⁵⁸, H. Yu¹², S. Yuan²⁰, A. Yuncu ⁹⁴, V. Zaccolo ²³, C. Zampolli ³², F. Zanone ⁹⁴, N. Zardoshti ³², A. Zarochentsev ¹⁴⁰, P. Závada ⁶², N. Zaviyalov ¹⁴⁰, M. Zhalov ¹⁴⁰, B. Zhang ^{94,6}, C. Zhang ¹³⁰, L. Zhang ³⁹, M. Zhang ^{127,6}, M. Zhang ⁶, S. Zhang ³⁹, X. Zhang ⁶, Y. Zhang¹²⁰, Z. Zhang ⁶, M. Zhao ¹⁰, V. Zhrebchevskii ¹⁴⁰, Y. Zhi¹⁰, D. Zhou ⁶, Y. Zhou ⁸³, J. Zhu ^{54,6}, S. Zhu¹²⁰, Y. Zhu⁶, S.C. Zugravel ⁵⁶, N. Zurlo ^{134,55}

Affiliation Notes

^I Deceased

^{II} Also at: Max-Planck-Institut fur Physik, Munich, Germany

^{III} Also at: Italian National Agency for New Technologies, Energy and Sustainable Economic Development (ENEA), Bologna, Italy

^{IV} Also at: Dipartimento DET del Politecnico di Torino, Turin, Italy

^V Also at: Yildiz Technical University, Istanbul, Türkiye

^{VI} Also at: Department of Applied Physics, Aligarh Muslim University, Aligarh, India

^{VII} Also at: Institute of Theoretical Physics, University of Wroclaw, Poland

^{VIII} Also at: An institution covered by a cooperation agreement with CERN

Collaboration Institutes

¹ A.I. Alikhanyan National Science Laboratory (Yerevan Physics Institute) Foundation, Yerevan, Armenia

² AGH University of Krakow, Cracow, Poland

³ Bogolyubov Institute for Theoretical Physics, National Academy of Sciences of Ukraine, Kiev, Ukraine

⁴ Bose Institute, Department of Physics and Centre for Astroparticle Physics and Space Science (CAPSS), Kolkata, India

⁵ California Polytechnic State University, San Luis Obispo, California, United States

⁶ Central China Normal University, Wuhan, China

⁷ Centro de Aplicaciones Tecnológicas y Desarrollo Nuclear (CEADEN), Havana, Cuba

⁸ Centro de Investigación y de Estudios Avanzados (CINVESTAV), Mexico City and Mérida, Mexico

⁹ Chicago State University, Chicago, Illinois, United States

¹⁰ China Institute of Atomic Energy, Beijing, China

¹¹ China University of Geosciences, Wuhan, China

¹² Chungbuk National University, Cheongju, Republic of Korea

¹³ Comenius University Bratislava, Faculty of Mathematics, Physics and Informatics, Bratislava, Slovak Republic

¹⁴ Creighton University, Omaha, Nebraska, United States

¹⁵ Department of Physics, Aligarh Muslim University, Aligarh, India

¹⁶ Department of Physics, Pusan National University, Pusan, Republic of Korea

¹⁷ Department of Physics, Sejong University, Seoul, Republic of Korea

¹⁸ Department of Physics, University of California, Berkeley, California, United States

¹⁹ Department of Physics, University of Oslo, Oslo, Norway

²⁰ Department of Physics and Technology, University of Bergen, Bergen, Norway

²¹ Dipartimento di Fisica, Università di Pavia, Pavia, Italy

²² Dipartimento di Fisica dell'Università and Sezione INFN, Cagliari, Italy

²³ Dipartimento di Fisica dell'Università and Sezione INFN, Trieste, Italy

²⁴ Dipartimento di Fisica dell'Università and Sezione INFN, Turin, Italy

²⁵ Dipartimento di Fisica e Astronomia dell'Università and Sezione INFN, Bologna, Italy

²⁶ Dipartimento di Fisica e Astronomia dell'Università and Sezione INFN, Catania, Italy

²⁷ Dipartimento di Fisica e Astronomia dell'Università and Sezione INFN, Padova, Italy

²⁸ Dipartimento di Fisica ‘E.R. Caianiello’ dell’Università and Gruppo Collegato INFN, Salerno, Italy

²⁹ Dipartimento DISAT del Politecnico and Sezione INFN, Turin, Italy

³⁰ Dipartimento di Scienze MIFT, Università di Messina, Messina, Italy

³¹ Dipartimento Interateneo di Fisica ‘M. Merlin’ and Sezione INFN, Bari, Italy

- ³² European Organization for Nuclear Research (CERN), Geneva, Switzerland
³³ Faculty of Electrical Engineering, Mechanical Engineering and Naval Architecture, University of Split, Split, Croatia
³⁴ Faculty of Engineering and Science, Western Norway University of Applied Sciences, Bergen, Norway
³⁵ Faculty of Nuclear Sciences and Physical Engineering, Czech Technical University in Prague, Prague, Czech Republic
³⁶ Faculty of Physics, Sofia University, Sofia, Bulgaria
³⁷ Faculty of Science, P.J. Šafárik University, Košice, Slovak Republic
³⁸ Frankfurt Institute for Advanced Studies, Johann Wolfgang Goethe-Universität Frankfurt, Frankfurt, Germany
³⁹ Fudan University, Shanghai, China
⁴⁰ Gangneung-Wonju National University, Gangneung, Republic of Korea
⁴¹ Gauhati University, Department of Physics, Guwahati, India
⁴² Helmholtz-Institut für Strahlen- und Kernphysik, Rheinische Friedrich-Wilhelms-Universität Bonn, Bonn, Germany
⁴³ Helsinki Institute of Physics (HIP), Helsinki, Finland
⁴⁴ High Energy Physics Group, Universidad Autónoma de Puebla, Puebla, Mexico
⁴⁵ Horia Hulubei National Institute of Physics and Nuclear Engineering, Bucharest, Romania
⁴⁶ HUN-REN Wigner Research Centre for Physics, Budapest, Hungary
⁴⁷ Indian Institute of Technology Bombay (IIT), Mumbai, India
⁴⁸ Indian Institute of Technology Indore, Indore, India
⁴⁹ INFN, Laboratori Nazionali di Frascati, Frascati, Italy
⁵⁰ INFN, Sezione di Bari, Bari, Italy
⁵¹ INFN, Sezione di Bologna, Bologna, Italy
⁵² INFN, Sezione di Cagliari, Cagliari, Italy
⁵³ INFN, Sezione di Catania, Catania, Italy
⁵⁴ INFN, Sezione di Padova, Padova, Italy
⁵⁵ INFN, Sezione di Pavia, Pavia, Italy
⁵⁶ INFN, Sezione di Torino, Turin, Italy
⁵⁷ INFN, Sezione di Trieste, Trieste, Italy
⁵⁸ Inha University, Incheon, Republic of Korea
⁵⁹ Institute for Gravitational and Subatomic Physics (GRASP), Utrecht University/Nikhef, Utrecht, Netherlands
⁶⁰ Institute of Experimental Physics, Slovak Academy of Sciences, Košice, Slovak Republic
⁶¹ Institute of Physics, Homi Bhabha National Institute, Bhubaneswar, India
⁶² Institute of Physics of the Czech Academy of Sciences, Prague, Czech Republic
⁶³ Institute of Space Science (ISS), Bucharest, Romania
⁶⁴ Institut für Kernphysik, Johann Wolfgang Goethe-Universität Frankfurt, Frankfurt, Germany
⁶⁵ Instituto de Ciencias Nucleares, Universidad Nacional Autónoma de México, Mexico City, Mexico
⁶⁶ Instituto de Física, Universidade Federal do Rio Grande do Sul (UFRGS), Porto Alegre, Brazil
⁶⁷ Instituto de Física, Universidad Nacional Autónoma de México, Mexico City, Mexico
⁶⁸ iThemba LABS, National Research Foundation, Somerset West, South Africa
⁶⁹ Jeonbuk National University, Jeonju, Republic of Korea
⁷⁰ Johann-Wolfgang-Goethe Universität Frankfurt Institut für Informatik, Fachbereich Informatik und Mathematik, Frankfurt, Germany
⁷¹ Korea Institute of Science and Technology Information, Daejeon, Republic of Korea
⁷² KTO Karatay University, Konya, Turkey
⁷³ Laboratoire de Physique Subatomique et de Cosmologie, Université Grenoble-Alpes, CNRS-IN2P3, Grenoble, France
⁷⁴ Lawrence Berkeley National Laboratory, Berkeley, California, United States
⁷⁵ Lund University Department of Physics, Division of Particle Physics, Lund, Sweden
⁷⁶ Nagasaki Institute of Applied Science, Nagasaki, Japan
⁷⁷ Nara Women's University (NWU), Nara, Japan
⁷⁸ National and Kapodistrian University of Athens, School of Science, Department of Physics , Athens, Greece
⁷⁹ National Centre for Nuclear Research, Warsaw, Poland
⁸⁰ National Institute of Science Education and Research, Homi Bhabha National Institute, Jatni, India
⁸¹ National Nuclear Research Center, Baku, Azerbaijan
⁸² National Research and Innovation Agency - BRIN, Jakarta, Indonesia

- ⁸³ Niels Bohr Institute, University of Copenhagen, Copenhagen, Denmark
⁸⁴ Nikhef, National institute for subatomic physics, Amsterdam, Netherlands
⁸⁵ Nuclear Physics Group, STFC Daresbury Laboratory, Daresbury, United Kingdom
⁸⁶ Nuclear Physics Institute of the Czech Academy of Sciences, Husinec-Řež, Czech Republic
⁸⁷ Oak Ridge National Laboratory, Oak Ridge, Tennessee, United States
⁸⁸ Ohio State University, Columbus, Ohio, United States
⁸⁹ Physics department, Faculty of science, University of Zagreb, Zagreb, Croatia
⁹⁰ Physics Department, Panjab University, Chandigarh, India
⁹¹ Physics Department, University of Jammu, Jammu, India
⁹² Physics Program and International Institute for Sustainability with Knotted Chiral Meta Matter (SKCM2), Hiroshima University, Hiroshima, Japan
⁹³ Physikalisches Institut, Eberhard-Karls-Universität Tübingen, Tübingen, Germany
⁹⁴ Physikalisches Institut, Ruprecht-Karls-Universität Heidelberg, Heidelberg, Germany
⁹⁵ Physik Department, Technische Universität München, Munich, Germany
⁹⁶ Politecnico di Bari and Sezione INFN, Bari, Italy
⁹⁷ Research Division and ExtreMe Matter Institute EMMI, GSI Helmholtzzentrum für Schwerionenforschung GmbH, Darmstadt, Germany
⁹⁸ Saga University, Saga, Japan
⁹⁹ Saha Institute of Nuclear Physics, Homi Bhabha National Institute, Kolkata, India
¹⁰⁰ School of Physics and Astronomy, University of Birmingham, Birmingham, United Kingdom
¹⁰¹ Sección Física, Departamento de Ciencias, Pontificia Universidad Católica del Perú, Lima, Peru
¹⁰² Stefan Meyer Institut für Subatomare Physik (SMI), Vienna, Austria
¹⁰³ SUBATECH, IMT Atlantique, Nantes Université, CNRS-IN2P3, Nantes, France
¹⁰⁴ Sungkyunkwan University, Suwon City, Republic of Korea
¹⁰⁵ Suranaree University of Technology, Nakhon Ratchasima, Thailand
¹⁰⁶ Technical University of Košice, Košice, Slovak Republic
¹⁰⁷ The Henryk Niewodniczanski Institute of Nuclear Physics, Polish Academy of Sciences, Cracow, Poland
¹⁰⁸ The University of Texas at Austin, Austin, Texas, United States
¹⁰⁹ Universidad Autónoma de Sinaloa, Culiacán, Mexico
¹¹⁰ Universidade de São Paulo (USP), São Paulo, Brazil
¹¹¹ Universidade Estadual de Campinas (UNICAMP), Campinas, Brazil
¹¹² Universidade Federal do ABC, Santo Andre, Brazil
¹¹³ Universitatea Națională de Știință și Tehnologie Politehnica Bucuresti, Bucharest, Romania
¹¹⁴ University of Cape Town, Cape Town, South Africa
¹¹⁵ University of Derby, Derby, United Kingdom
¹¹⁶ University of Houston, Houston, Texas, United States
¹¹⁷ University of Jyväskylä, Jyväskylä, Finland
¹¹⁸ University of Kansas, Lawrence, Kansas, United States
¹¹⁹ University of Liverpool, Liverpool, United Kingdom
¹²⁰ University of Science and Technology of China, Hefei, China
¹²¹ University of South-Eastern Norway, Kongsberg, Norway
¹²² University of Tennessee, Knoxville, Tennessee, United States
¹²³ University of the Witwatersrand, Johannesburg, South Africa
¹²⁴ University of Tokyo, Tokyo, Japan
¹²⁵ University of Tsukuba, Tsukuba, Japan
¹²⁶ Universität Münster, Institut für Kernphysik, Münster, Germany
¹²⁷ Université Clermont Auvergne, CNRS/IN2P3, LPC, Clermont-Ferrand, France
¹²⁸ Université de Lyon, CNRS/IN2P3, Institut de Physique des 2 Infinis de Lyon, Lyon, France
¹²⁹ Université de Strasbourg, CNRS, IPHC UMR 7178, F-67000 Strasbourg, France, Strasbourg, France
¹³⁰ Université Paris-Saclay, Centre d'Etudes de Saclay (CEA), IRFU, Département de Physique Nucléaire (DPhN), Saclay, France
¹³¹ Université Paris-Saclay, CNRS/IN2P3, IJCLab, Orsay, France
¹³² Università degli Studi di Foggia, Foggia, Italy
¹³³ Università del Piemonte Orientale, Vercelli, Italy
¹³⁴ Università di Brescia, Brescia, Italy
¹³⁵ Variable Energy Cyclotron Centre, Homi Bhabha National Institute, Kolkata, India

¹³⁶ Warsaw University of Technology, Warsaw, Poland

¹³⁷ Wayne State University, Detroit, Michigan, United States

¹³⁸ Yale University, New Haven, Connecticut, United States

¹³⁹ Yonsei University, Seoul, Republic of Korea

¹⁴⁰ Affiliated with an institute covered by a cooperation agreement with CERN

¹⁴¹ Affiliated with an international laboratory covered by a cooperation agreement with CERN.